Discovery and isolation of novel capsaicinoids and their TRPV1-related activity

Authors

Joshua David Smith[1,2,&], Vendula Tvrdoňová Stillerová[3,&], Martin Dračinský[1], Hannah Lovinda Angermeier Gaustad[1], Quentin Lorenzi[1], Helena Smrčková[1], Jakob K. Reinhardt[4,5], Marjorie Anne Liénard[6,7], Lucie Bednárová[1], Pavel Šácha[1], Tomáš Pluskal[1,*]

[1]Institute of Organic Chemistry and Biochemistry of the Czech Academy of Sciences, Prague, Czechia, [2]First Faculty of Medicine Charles University, Prague, Czechia, [3]CZ-OPENSCREEN, Institute of Molecular Genetics of the Czech Academy of Science, Prague, Czechia, [4]Department of Pharmaceutical Sciences, University of Basel, Switzerland, [5]Chemistry & Chemical Biology of Northeastern University, Boston, USA, [6]Broad Institute, Boston, USA,[7]GIGA Institute, University of Liège, Liège, Belgium

& J.D.S. and V.T.S. contributed equally to this work.
*To whom correspondence may be addressed. Email: tomas.pluskal@uochb.cas.cz

Keywords: natural products, vanilloids, capsaicin, MS/MS spectrometry, calcium imaging, TRPV1, metabolomics

Abstract

Chilis contain capsaicin, an acclaimed molecule in both science and culinary ventures. Capsaicin's target protein, the transient receptor potential cation channel subfamily V member 1 (TRPV1), has been linked to many post-activation effects, including changes in metabolism and pain sensation. Beneficial effects of TRPV1 activation by capsaicin have been explored through clinical trials. Capsaicinoids other than capsaicin also bind to TRPV1, but current studies often disregard non-capsaicin interactions. To fill in these gaps, we screened 40 different chili varieties derived from four *Capsicum* species by means of untargeted metabolomics and a rat TRPV1 (rTRPV1) calcium influx activation assay. The resulting capsaicinoid profiles were specific to each variety but only partially corresponded with species delimitations. Based on rTRPV1 activation elicited by crude chili extracts, capsaicinoids act in a synergistic manner and a capsaicinoid profile can serve as a gauge of this activation. In addition, we isolated eighteen capsaicinoids, including five previously unreported ones, and confirmed their structure by NMR and MS/MS. We then tested rTRPV1 activation by 23 capsaicinoids and three related

compounds. This testing revealed that even slight deviations from the structure of capsaicin reduce the ability to activate the target, with a mere single hydroxylation on the acyl tail reducing potency towards rTRPV1 by more than 100-fold. In addition, we tested how rTRPV1 activity changes in the presence of capsaicin together with non-activating capsaicin analogs and weakly activating capsaicinoids and found both classes of molecules to positively modulate the effects of capsaicin. This demonstrates that even such compounds have measurable pharmacological effects, making a case for the use and study of natural chili extracts.

Introduction

Chilis are a broad term for variously spicy fruits produced by different species of *Capsicum.* There are 26 known species of chili peppers with many varieties and cultivars, but only five species have been domesticated: *C. annuum* L. var. *annuum*, *C. chinense* Jacq., *C. frutescens* L., *C. baccatum* L. var. *pendulum* (Willd.) Eshbaugh and *C. pubescens* L. *(1)*. Some of the world's hottest chilis, such as habanero, Carolina Reaper and Pepper X, are varieties of the species *C. chinense*. At the time of our study, Carolina Reaper was established as the spiciest pepper in the world, but it has since been dethroned by Pepper X (2). Chilis are ranked based on a measurement system called the Scoville scale, which originally utilized human taste subjected to series of sugar and ethanol dilutions of chili pepper extracts; the number of dilutions needed to neutralize the spice were reported as the number of Scoville Heat Units (SHU) (3). Currently, Scoville measurements are typically conducted by determining the content of capsaicin and dihydrocapsaicin using high-performance liquid chromatography (HPLC) or gas chromatography (4, 5). Modern computational metabolomics allows for more thorough investigations of biological samples compared to traditional MS analysis. In particular, untargeted metabolomics has burgeoned in the past decade with the development of computational tools such as MZmine, SIRIUS and GNPS. (6) (7) (8). Despite these technological advancements, capsaicinoids have so far been investigated only in a targeted manner.

Capsaicin and dihydrocapsaicin are typically the two most abundant capsaicinoids found in chili; however, inconsistencies across varieties have been reported (9). All capsaicinoids share a common structural scaffold consisting of a vanilloid head attached via an amine bond ("neck") to an acyl tail of varying length (Fig. 1). To date, about 25 different capsaicinoids have been reported (Fig. 1 and Supplementary Table 1). For some of these compounds, only tentative structures without NMR confirmation are available or have been published without corresponding NMR spectra (10, 11). Therefore, not all data regarding capsaicinoids are up to current "FAIR – Findable, Accessible, Interoperable, and Reusable" standards (12).

Chili extracts are offered as over-the-counter dietary supplements, as well as analgesic creams and patches containing varied mixtures of capsaicinoids. Most studies involving capsaicinoids, however, have focused solely on capsaicin or dihydrocapsaicin (13–15), which limits our understanding of how capsaicinoids function as a group. The relevance of this understanding is

exemplified in *Capsicum* extracts administered in clinical trials, for example NCT06363305 or NCT03489226 (16, 17). Capsaicinoids have been of relevance due to their ability to bind to the transient receptor potential cation channel subfamily V member 1 protein (TRPV1), found in nociceptive neurons (18). TRPV1 is a homotetramer membrane channel activated by voltage, heat, capsaicin and double-knot toxin, where each of these stimulants have their own activating part(19, 20). Capsaicin binding pocket is surrounded by helixes S4, S6 and S4-S5 linker. When capsaicin binds to TRPV1, the channel transition starts by gating and follows to selectivity filter (21–23). Once the channel is fully activated resulting in a flux of cations, preferentially sodium and calcium, causing a plethora of downstream biological effects, including a sensation of pain and heat (24, 25).

Despite the use of chili extracts in over-the-counter products and in clinical trials, we have a relatively limited understanding of how extracts from different *Capsicum* varieties, containing diverse mixtures of capsaicinoids, can influence TRPV1 activity. Furthermore, many identified capsaicinoids have not been individually tested for their effects on TRPV1. We therefore set out to examine how different capsaicinoid profiles and individual capsaicinoids influence TRPV1 activation. In addition, suspecting that the breeding of ever-hotter varieties might have resulted in TRPV1 agonists even more potent than capsaicin or dihydrocapsaicin, we performed an untargeted metabolomic screening of 40 different chili samples in a rTRPV1 activation assay.

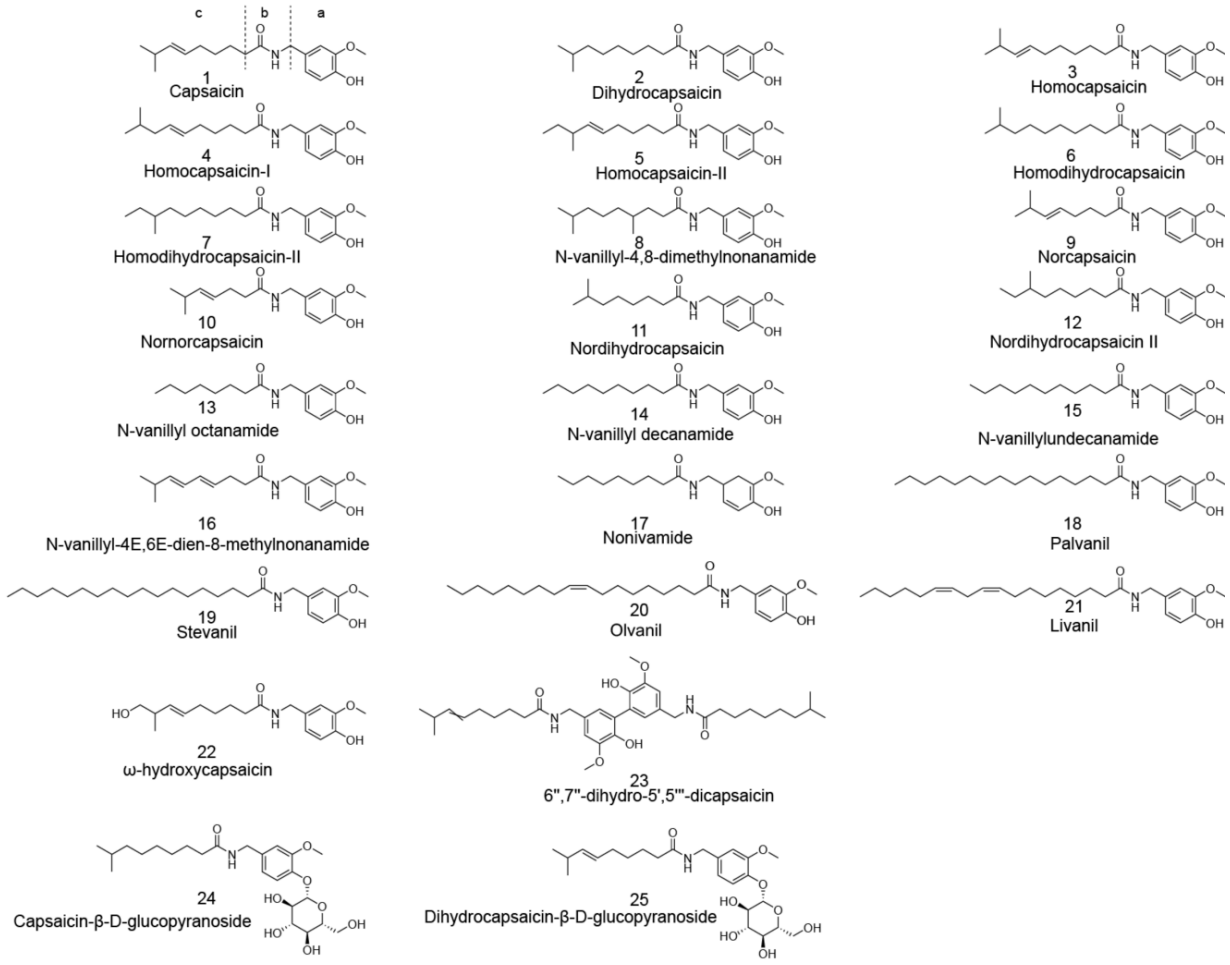

Fig.1. Previously isolated capsaicinoids. All capsaicinoids can be divided into three parts (highlighted on compound 1 – capsaicin): a – vanilloid head; b – amide bond (neck) region; and c – alkyl tail (26).

Results and Discussion

Untargeted metabolomics of chili varieties reveals novel candidate capsaicinoids

To explore the chemical space of capsaicinoids contained in chili peppers, we performed an untargeted metabolomic investigation of 40 chili varieties covering a wide range of heat levels (Table 1), which are in long-term cultivation at the Botanical Garden of the Faculty of Tropical AgriSciences of the Czech University of Life Sciences in Prague.

Table 1. Summary of chili varieties analyzed in the present study, their species identity and informational numbers of Scoville Units[1].

	Common Name	Species	Scoville Units (SHU)
1	Lemon Drop	*Capsicum baccatum*	15,000–30,000
2	Escabeche	*C. baccatum*	12,000–17,000
3	Capsaicum.B	*C. baccatum*	≤ 200,000
4	Pimenta Trepaderra de Werner	*C. baccatum*	70,000–100,000
5	Glocken	*C. baccatum*	5,000–30,000
6	Criolla Sella	*C. baccatum*	25,000–30,000
7	Black Prince	*C. annuum*	10,000–30,000
8	Thai Culinary Hot†	*C. annuum*	25,000–40,000
9	Fish Pepper	*C. annuum*	5,000–30,000
10	Chips	*C. annuum*	N/A
11	Hot Fish	*C. annuum*	10,000–20,000
12	Sahuaro	*C. annuum*	500
13	Trinidad Moruga Scorpion*	*C. chinense*	800,000–1,000,000
14	Brasilian Hot Bonnet	*C. chinense*	100,000–350,000
15	Habanero	*C. chinense*	100,000–350,000
16	Naga Morich*	*C. chinense*	≤ 1,040,000
17	Dorset Naga†	*C. chinense*	1,000,000–1,500,000
18	Chilhuacle	*C. annuum*	5,000–15,000
19	Pendulum	*C. baccatum*	5,000–15,000
20	Peri Peri	*C. frutescens*	30,000–100,000
21	Hungarian Black	*C. annuum*	500–2,500
22	African Bird's Eye Chili	*C. frutescens*	80,000–150,000
23	Jalapeno Summer Heat†	*C. annuum*	10,000
24	Bolivian Rainbow	*C. annuum*	10,000–30,000
25	Miniature Chocolate Bell	*C. annuum*	0
26	Vezena Piperka	*C. annuum*	≤ 10,000

27	Carolina Reaper*,†	*C. chinense*	1,150,000–2,200,000
28	Habanero Madame Jeanette	*C. chinense*	100,000–350,000
29	Habanero White Long	*C. chinense*	≤ 300,000
30	7 Pot Brain Yellow	*C. chinense*	≤ 1,400,000
31	Trinidad Congo Red*,†	*C. chinense*	250,000–350,000
32	Limon	*C. chinense*	15 000–30 000
33	Trinidad Congo Yellow*	*C. chinense*	100,000–350,000
34	Trinidad Scorpion Butch T*,†	*C. chinense*	1,000,000–1,500,000
35	Naga Bhut Jolokia	*C. chinense*	≤ 1,000,000
36	Jamaican Hot Yellow†	*C. chinense*	≤ 100,000
37	Chocolate Habanero	*C. chinense*	≤ 500,000
38	Habanero White†	*C. chinense*	300,000–450,000
39	Fatalii White†	*C. chinense*	125,000–325,000
40	Habanero Large Brown*	*C. chinense*	100,000–350,000

*:Samples used in the first large-scale extraction

†:Samples used in the second large-scale extraction

[1]The values of Scoville Units presented in this table were obtained from either the Botanical Garden of the Faculty of Tropical AgriSciences of the Czech University of Life Sciences in Prague or an established chili dealer. Capsaicinoid profiles and how they are measured when determining the Scoville Units (27) are susceptible to many factors of variance. Ultimately, Scoville Units are never absolute and are only a way to roughly gauge a variety's heat level.

SIRIUS and CANOPUS investigation of data based on predicted compound classes

Despite extensive research in the area, studies on capsaicinoids have mostly been limited to targeted analysis of already known compounds (28–32). To start exploring the chemical space and distribution of capsaicinoids amongst different chili varieties, and to explain differences in TRPV1 activation observed between varieties we first screened 40 chili varieties,listed in Table 1, in an untargeted manner by means of UHPLC–MS/MS (Fig. 2*A*). To obtain a holistic understanding of the chili metabolome, we then leveraged MZmine for raw data processing and "feature-finding"(i.e. feature–a "meaningful" MS signal produced by a small molecule occurring the the sample)(6, 33), GNPS for feature-based molecular networking (7), and SIRIUS for feature annotation. To help identify capsaicinoids, we used CANOPUS, a part of SIRIUS, which allows for compound class prediction and SIRIUS molecular formula prediction (34, 35). Results from CANOPUS indicated "n-acyl amines" as the largest compound class that accounted for 12.3% percent of all features found across all varieties (Fig. 2*B*). N-acyl amines are the necessary precursors to the acyl moieties of all capsaicinoids (Fig. 1). By contrast, features predicted to be phenylethylamines, simple phenolic acids and derivatives of cinnamic acid, such as the capsaicinoid precursors vanillylamine and vanillin, accounted for about 1–2% of all features. Furthermore, we did not detect vanillylamine in any chili sample. It has been reported that low levels of phenylethylamines are due to their quick conversion into capsaicinoids (36). The excess of n-acyl amines could further indicate that these phenylethylamines are a limiting factor in capsaicinoid biosynthesis. As expected, capsaicinoids were one the largest predicted

classes of molecules at 6.85% (Fig. 2*B*). Other major compound classes present are not considered in this paper.

The initial screening of 40 chili varieties revealed only 1530 features, which is a relatively small number for that amount of samples, indicating that many features are shared by the varieties. However, there was no discernible intraspecies clustering based on capsaicinoids profiles and the hierarchical clustering of metabolomic features (Fig. 2*C*). One example that highlights this irregular pattern is the variety Lemon Drop, which contains more dihydrocapsaicin than capsaicin. This observation is consistent with previous targeted capsaicinoid experiments, which indicated that the composition of capsaicinoids is not a good chemotaxonomic identifier (9) and was specific to each variety.

Exploration for novel capsaicinoids and capsinoids

Contrary to expectation, however, we found no capsiate or other capsinoid in our initial screening. Capsiate is a non-pungent analog of capsaicin found in *Capsicum annuum* (Fig. S2, compound **39**) (37). The main difference between the two molecules lies in their precursors, which are vanillyl alcohol and vanillylamine, respectively (38). The chilis we screened included only one non-pungent variety and several less spicy varieties of *Capsicum annuum*. The analyzed fruit extracts likely lack the pAMT mutation needed for the production of vanillyl alcohol (39) and capsinoid production.

To identify possible novel capsaicinoids, we constructed a feature-based molecular network on the GNPS platform, which groups clusters of molecules based on similarities in their MS/MS (Fig. 2*D and S3*). Capsaicinoids are identifiable by CANOPUS molecular class annotation and verifiable based on the presence of capsaicin and other nodes with the vanilloid head MS/MS fragment of m/z = 137 (29). Using this network, we selected several targets for isolation based on mass or fragmentation indicative of hydroxylation, tail length, or dimerization, assuming that the target compounds would produce a spectrum of TRPV1 activation.

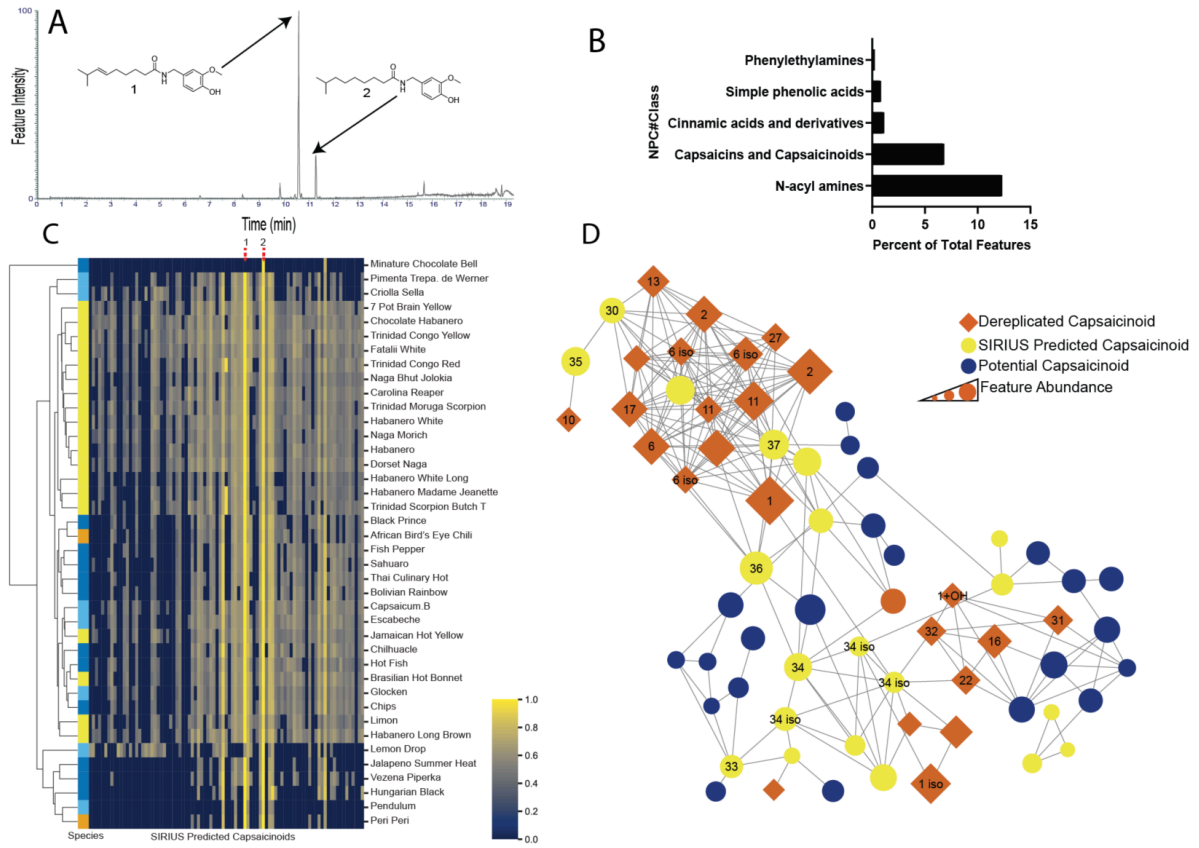

Fig.2. Untargeted metabolomic analysis highlighting features related to capsaicinoid composition. (A) Representative example trace of an LC–MS base peak chromatogram of a Carolina Reaper extract. (B) Top five molecular classes predicted by SIRIUS based on the MS data of crude extracts. (C) Clustering and heatmap of all capsaicinoid-like compounds predicted by SIRIUS, capsaicin **1** and dihydrocapsaicin **2** are highlighted. Features predicted to be characteristic of capsaicinoids were reduced to their $\log_{10}$ values and then normalized by rows to the most abundant feature per variety. Species are color-coded as follows: yellow (#F0E442) – *C. chinense*, blue (#0072B2) – *C. annuum*, sky blue (#56B4E9) – *C. baccatum*, orange (#E69F00) – *C. frutescens*. (D) Main capsaicinoid network based on all 40 varieties. Most labeled nodes are confirmed using reference standards with retention time (RT). Dereplicated nodes are features with predicted chemical formulas matching the chemical formulas of known capsaicinoids. Some nodes are labeled **iso**, meaning they have an MS/MS match for the same compound but have a different RT. Other molecules marked with **+OH** are indicative of hydroxylation. The strong homology of these compounds highlights the importance of having either a standard or NMR data for structure confirmation. Compounds denoted as potential capsaicinoids contained fragments indicative of a vanilloid head but were not predicted to be capsaicinoids by CANOPUS.

Isolation and purification of capsaicinoids resulted in 5 novel structures

In order to investigate the effects of both crude extracts and individual capsaicinoids on the TRPV1 receptor, we proceeded to purify the target compounds from our initial screening. To do so, a pooled selection of lyophilized chilis were macerated in ethyl acetate and pre-fractionated by flash-chromatography prior to the isolation of individual compounds using semi-preparative HPLC (Fig. 3*A and* 3*B*). In total, we isolated 18 capsaicinoids, including five novel molecules and several others that were previously only obtained through synthesis (Fig. 3*C* and Table 2). Information about the MS/MS fragmentation of each isolated compound can be found in Supplementary File S1, and NMR data are provided in Supplementary File S2.

Table 2. Summary of isolated capsaicinoids; RT – LC-MS retention time, Base peak m/z $[M+H]^+$ – base peak mass, UV_{max} – maximum UV absorbance

Compound number	**Compound name**	**Amount [mg]**	**Description**	**RT**	**Base peak m/z $[M+H]^+$**	**UV_{max}**
10	Nornorcapsaicin	0.24	Yellow-orange residue	8.93	278.1749	283.5
13	N-vanillyl octanamide	1.13	Yellow oily residue	9.67	280.1906	284
16	N-vanillyl-4E,6E-dien-8-methylnonanamide	1.29	Yellow oily residue	10.09	304.1908	247
22	ω-hydroxycapsaicin	0.43	Yellow residue	7.18	322.2016	284
23	5,5′-di-capsaicin-dihydrocapsaicin	0.62	Yellow residue	13.88	611.4063	247
26	N-heptanoate vanillylamide	0.22	White residue	8.72	266.1748	243.5
27	Nornordihydrocapsaicin	0.28	White residue	9.50	280.1906	284
28	N-vanillylbutyramide*	0.40	White residue	5.43/5.48	224.1280	244.5
29	N-vanillyl-isobutyramide*	0.40	White residue	5.43/5.48	224.1280	244.5
30	N-Isovalerylvanillylamin	0.51	Yellow residue	6.40	238.1436	284
31	N-(4-hydroxy-3-methoxybenzyl)-8-methyl-7-oxononanamide	0.55	Yellow residue	7.94	322.2014	283.5
32	Epicapsaicin	0.26	Yellow residue	8.08	322.2017	284.5

33	N-vanillyl-9-hydroxydecanamide†	0.41	Yellow residue	7.35	324.2169	284
34	N-vanillyl-7-hydroxy-8-methylnonamide†	0.87	Yellow residue	7.66	324.2170	284
35	N-vanillyl 6-Methyl-2,4-heptadienamide†	0.31	Yellow residue	9.03	276.1595	258.5
36	N-vanillyl-capsaicin ether†	< 1.0	Yellow residue	11.58	442.2591	N/A
37	N-vanillyl-dihydrocapsaicin ether†	< 1.0	Yellow residue	12.19	444.2745	N/A
38	5,5′-dicapsaicin	0.21	Yellow residue	13.37	609.3901	243.5

*Compounds were isolated in a mixture.
†:Novel capsaicinoids

We successfully annotated, with a high degree of confidence, 26 out of 50 nodes (52%) predicted to be capsaicinoids in our final network of pooled chilis by comparing the retention times and characteristic ions of isolated compounds with those of purchased reference standards (capsaicinoids **1**, **2**, **4**, **11**, **14**, **17**, **20** and **24**) (Fig. 2*D*). Nodes predicted to be capsaicinoids that are left unannotated correspond to substances of varying tail length or differing in hydroxylation. We removed all redundant adducts and other artifacts from the network (Fig. S4).

Among those, capsaicinoids **10**, **13** and **26–30** with varying tail length were expected based on SIRIUS formula prediction and manual inspection of MS/MS spectra. Capsaicinoids **10** and **13** were previously reported (40, 41). Interestingly, capsaicinoids **26**, **29** and **30** have only been chemically synthesized and have never been isolated from a chili species (21, 42, 43) whereas capsaicinoid **28** has only been enzymatically synthesized (37). Capsaicinoid **27** has been synthesized and only tentatively isolated from *C. chinense* and *C.annuum* without any NMR or reference standard confirmation (15, 44–46).

Capsaicinoids **22**, **31**, **32**, **33**, **34** are tail-oxidized. ω-Hydroxycapsaicin, capsaicinoid **22**, was first identified as a microbial metabolite (47), later isolated from *C.annuum* (48) and then as a product of capsaicin p450 oxidation(49). Likewise, capsaicinoid **31** has previously been identified only as a product of human cell line oxidation, and capsaicinoid **32** has hitherto only been known as a product of microbial p450 enzyme catalysis and epiphytic processing (50–53). Lastly, to our knowledge, capsaicinoids **33** and **34** are reported here for the first time.

Only two capsaicinoids, **16** and **35**, were doubly reduced. Capsaicinoid **16** was isolated previously (41) whereas capsaicinoid **35** is a new structure first reported here.

Capsaicinoids **36** and **37** are both also newly identified and present a unique structure indicative of S_N2 chemistry on the vanilloid hydroxyl group. It is unlikely that capsaicinoids **36** and **37** are a photocatalyzed product, because these reactions typically result in insertion-like products, as seen in capsaicinoid **23**. The structure of capsaicinoid **36** was confirmed by NMR, which enabled us to determine capsaicinoid **37** by MS/MS analysis. Although both compounds can be isolated and were found in several harvests, they are markedly unstable based on repeated MS and NMR measurements. There were other nodes also indicative of possible acyl modifications to the vanillyl head of the capsaicin molecule, but these features were less pronounced and harder to generate a structure for with only MS/MS.

Two capsaicinoid dimers, **23** and **38,** were isolated. We obtained reliable NMR structural confirmation for 5,5'-dicapsaicin, capsaicinoid **38**. Capsaicinoid **23** was previously isolated from *C. annuum* (48) and was confirmed based on MS/MS differences compared to capsaicinoid **38**. Interestingly, capsaicinoid **38** has not been previously identified as a direct product of chili extraction. The first report of 5,5'-dicapsaicin was as a photocatalyzed dimer in the presence of riboflavin (54). The 5,5′-dicapsaicin dimer was also created using peroxidases extracted from *C. annuum* var. annuum fruits (55). Later, it was found that this molecule can also be formed through the radical-scavenging capabilities of capsaicin (56). The capsaicin dimer can also be a product of p450 oxidation (57, 58), and its formation has been observed by spiking capsaicin into a *C. annuum* var. *annuum* protein extract (59).

It was not possible to determine the absolute configuration of capsaicinoids with chiral centers, **22, 33** and **34,** using standard circular dichroism (CD) experiments. This inability to determine their absolute configuration was likely caused by the flexibility between the chromophore and the chiral center itself (60). Because of the limited amount of material available, CD spectroscopy structural assignment was not tested.

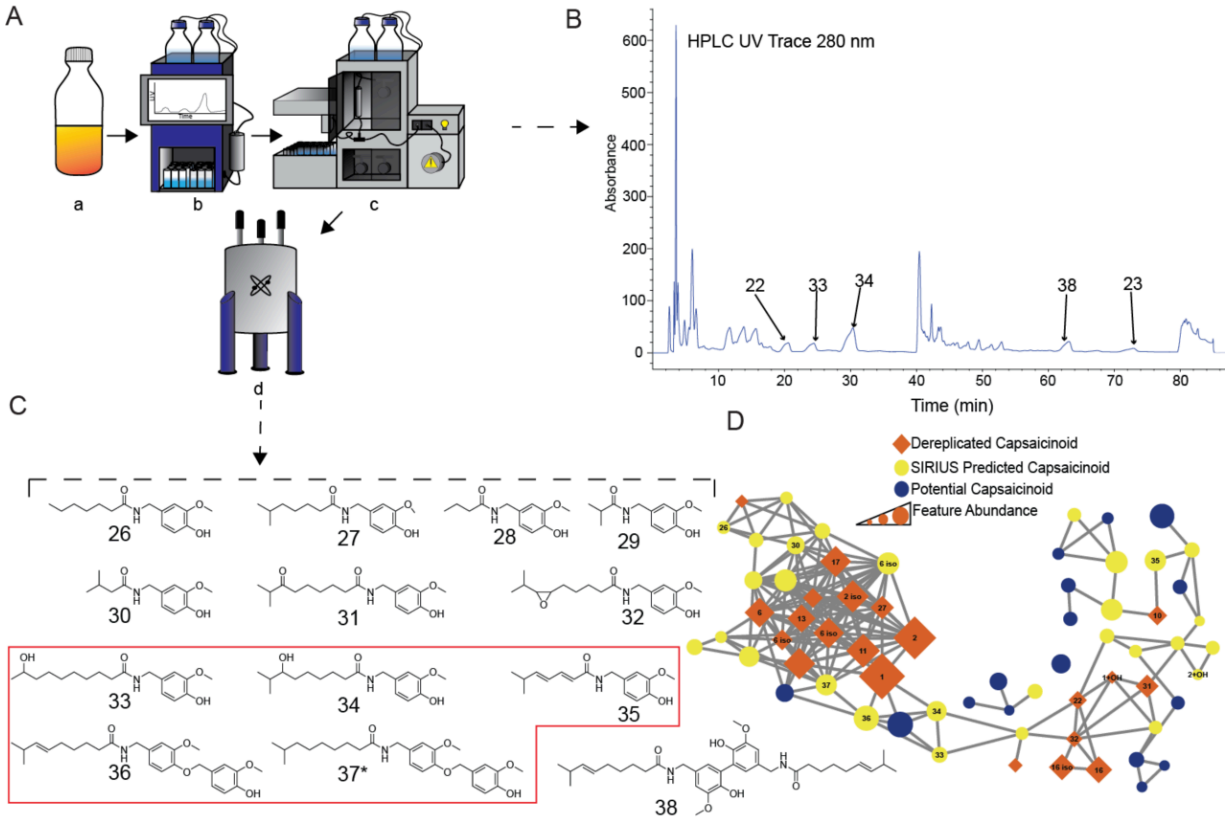

Fig. 3. *Isolation of capsaicinoids*. (A) Overall schema of the workflow: maceration (a) of chilis was followed by normal-phase flash-chromatography (b), isolation of individual compounds on HPLC (c) and lastly structure confirmation with NMR (d). (B) HPLC chromatogram from one of the pooled flash fractions highlighting the isolation of individual compounds. (C) Structures of newly isolated compounds.The red box highlights the novel capsaicinoids. *Compound **37** was identified based on the NMR structure of **36** followed by MS/MS analysis. (D) Molecular network used for compound identification before isolation. Most labeled nodes are nodes confirmed based on a reference standard or isolation. Some labeled nodes, such as **6 iso** or **1 + OH**, are nodes that had a library match to a compound with the same precursor match but a different retention time. The node corresponding to capsaicinoid **34** was identified as **33** with a .002 better cosine score; however, the retention time did not match. Capsaicinoids **28** and **29** were not in the initial network because of their low intensity, and dimers (**23** and **38**) were also in a separate network. Denoted as potential capsaicinoids are compounds that contain an MS/MS fragment indicative of a vanilloid head but predicted to be a different NPC class of capsaicinoids.

Capsaicinoids and related molecules modulate capsaicin induced TRPV1 activation

With the individual capsaicinoids at hand, we wanted to investigate the effects of both the isolated compounds and crude extracts on TRPV1 activation. Among laboratory model organisms, the human TRPV1 receptor (hTRPV1) shares the greatest degree of homology with the rat TRPV1 receptor (rTRPV1): 83% sequence similarity (61). In addition, rTRPV1 and hTRPv1 have been reported to have similar capsaicin-elicited activity, only rTRPV1 is less sensitive to capsazepine and ruthenium red, two common antagonists of TRPV1 (62). We used the Flp-In T-REx-293 cell line along with the rTRPV1 receptor and tetracycline repressor to create an inducible line denoted as irTRPV1-FlpIn293. Surface receptor expression was confirmed functionally (Fig. 4*C*) and by immunocytochemistry staining (Fig. S5). Our irTRPV1-FlpIn293 system under doxycycline control can express an excessive amount of receptors, which makes the sensitivity of our model close to that of radioactivity assays (18, 63).

Activation of rTRPV1 by crude chili extracts correlates with their capsaicinoid content
As stated in the previous section, we see that capsaicinoids are not a good taxonomic indicator; however, we were curious if there would be a relation between capsaicinoid composition and rTRPV1 activation. Indeed, our data revealed a strong correlation (Pearson = 0.89) between the capsaicinoid composition (i.e MS sum intensity of all capsaicinoid predicted features) of a given chili variety and the ED_{50} values of the corresponding crude extracts (Fig. 4*A*, Table S2). To see if capsaicin and dihydrocapsaicin were the driving force of this correlation, we removed these two substances from the sum intensity values (Fig. S6), but the correlation remained strong (Pearson = 0.77). This indicates that other capsaicinoids activate rTRPV1 in a synergistic manner. Hence, most extracts activated the receptor fully, and extracts S21, S22 and S24 also activated it, albeit partially. The crude extract from the chili variety Miniature Chocolate Bell (S25) elicited slight partial activation at the highest concentration tested, which may likely be caused by its lower capsaicinoid content (Table S2), although the presence of an inhibitor or negative modulator in the mixture cannot be ruled out. See Supplementary Table 2 for all values pertaining to crude extracts. Overall, this suggests that when considering chili spiciness all capsaicinoids present should be accounted for and not just a select few.

Overview of activity of the tested capsaicinoids and related compounds.
It is known that the vanilloid head of capsaicin is the most sensitive to atomic structure modification (64). In addition, modification to the neck can critically alter the recognition and potency of the compound (21, 65), as seen also with piperine (22, 66), gingerols (22, 67) and synthetic capsaicin analogs (65). It is also established that TRPV1 activation decreases as the tail of the capsaicinoid becomes shorter (21). Although these trends are known and many other synthetic agonists have been tested on TRPV1 (63, 68–70), there is still a large knowledge gap regarding the potency of naturally occurring capsaicinoids. We have filled this gap by testing 24 capsaicinoids and 3 other related compounds on rTRPV1 activation assay (Table 3).

Table 3

Overview of the potency of capsaicinoids isolated during this study. For more detailed data, refer to Supplementary Table 3.

Name	**Capsaicinoid number**	**EC_{50} [µM]**
Capsaicin	1	0.04
Dihydrocapsaicin	2	0.05
Homodihydrocapsaicin I	4	0.32
Nornorcapsaicin	10	0.81
Nordihydrocapsaicin	11	0.05
N-vanillyl octanamide	13	0.15
N-Vanillyldecanamide	14	0.20
N-vanillyl-4E,6E-dien-8-methylnonanamide	16	0.14
Nonivamide	17	0.18
Olvanil	20	0.12
ω-Hydroxycapsaicin	22	5.56
6″,7″-Dihydro-5′,5‴-dicapsaicin	23	10.27
Capsaicin β-D-glucopyranoside	24	4.69
N-Heptanoate vanillylamide	26	1.81
Nornordihydrocapsaicin	27	1.04
N-isovalerylvanillylamin	30	2.84
N-(4-Hydroxy-3-methoxybenzyl)-8-methyl-7-oxononanamide	31	0.56
Epicapsaicin	32	0.60
N-vanillyl-9-hydroxydecanamide	33	6.33
N-vanillyl-7-hydroxy-8-methylnonamide	34	1.46
N-vanillyl 6-Methyl-2,4-heptadienamide	35	1.20
5,5′-Dicapsaicin	38	4.46
Capsiate	39	490.90

Vanillin	40	n.d.
4-Hydroxy-3-methoxybenzyl alcohol	41	n.d.
N-Vanillylbutyramide / N-vanillyl-isobutyramide	28, 29	N.d

Of the 18 isolated compounds, only compounds **13**, **26** and **28** were, to the best of our knowledge, previously tested for TRPV1 activation (21). Of the purchased standards, other than capsaicin, capsaicinoids **2**, **17** and **20** were tested on dorsal root ganglia that express TRPV1, with respectively slightly higher EC_{50} values of 0.19 μM, 0.55 μM and 0.17 μM (71). Differences are explainable due to different testing systems. Capsaicinoids **14** and **17** were also previously tested, yielding EC_{50} values of 0.061 μM and 0.072 μM, respectively, in a $^{45}Ca^{2+}$ uptake assay utilizing rTRPV1-expressing Chinese hamster ovary cells (72). Our EC_{50} value for capsaicinoid **14** indicated almost three-fold lower potency, but within a range expected considering the differences in assay methods and expression systems. As far as we have been able to ascertain, no other capsaicinoid standards have been tested with a TRPV1 expression system.

Effect of tail modifications on rTRPV1 activation

Whereas the head is important for TRPV1 receptor gating, in both a positive(21–23) and negative(73, 74) manner, the exact length of the tail has been shown to have an effect on capsaicin's strong potency (21). The tail of capsaicin arrange for serie of van der Waal interactions with the S6 helix of capsaicin-binding pocket of TRPV1 receptor(21, 65, 75) follows after movement of the S4−S5 linker and the S6 helix caused by binding of vanilloid head (76). Compared to capsaicin, capsaicinoids **2**, **16** and **17** had the same number of carbons but differed either in their connectivity or in the number of hydrogens. Unsaturation, saturation or linearization of the tail, while maintaining the same number of carbons as capsaicin, only slightly reduced the potency of the molecule (Fig. 4*B* and 4*C*). Because the capsaicin tail interacts in the TRPV1 hydrophobic pocket through a series of van der Waals interactions, small losses of activity are consistent with small changes in carbon chain length and similar tail polarity. Capsaicinoids **22** and **31–34** also contained the same number of carbon atoms but were oxidized somewhere on the tail, and depending on the position of the oxygenation, EC_{50} values were reduced between 10- and 150-fold. Based on these results, any oxidative process, even on the tail, can be linked to lower TRPV1 activity. We attribute the reduction of potency due to tail-hydroxylation residing in a predominantly hydrophobic core and its interaction with the S6 helix. The pocket likely struggles to accommodate the polar oxygen and restricts the movement of the S6 helix upon vanilloid binding. Only three capsaicinoids, **4**, **11** and **17**, which differed by a single carbon atom, had similar EC_{50} values and were 1–6 times less potent than capsaicin. Nordihydrocapsaicin, **11**, had the most comparable TRPV1 activation concentration to capsaicin and dihydrocapsaicin of 0.05 μM (Fig. 4*B* and 4*C*).

Other capsaicinoids with 2–5 fewer carbons on the tail and those that had varying connectivity were markedly less potent than capsaicin, exhibiting 15-fold lower to almost zero activity. The sole exception, capsaicinoid **13**, N-vanillyl octanamide, was only about three times less potent

than capsaicin. Olvanil (**20**) and N-vanillylbutyramide/N-vanillyl-isobutyramide (**28** & **29**) both differed by six carbons. These three compounds were all partial agonists, but olvanil had a similar EC_{50} value to capsaicin (Fig. 4*B* and 4*C*). Short-tailed capsaicinoids have been investigated previously (21) and are known to be ineffective at opening TRPV1. Conversely, olvanil might be able to adopt a different position in which the binding of the vanilloid is less permissive due to the bulky tail interacting with the pulling of the S6 helix (65). The complete list of obtained EC_{50} values is in Table 3. The detailed dose–response curve data are presented in Supplementary Table 3. We further confirmed that the measured responses were due to rTRPV1 activation by using the competitive TRPV1 antagonist AMG-517 (77) (Fig. S7).

Modulation of rTRPV1 activity by not-potent capsaicinoids.
Capsaicin, other than in the form of an active ingredient, is always found in a mixture of capsaicinoids. The complexity of these mixtures varies from variety to variety and from extraction to extraction. We asked if capsaicinoids (Table 3, Fig. 4*A*) could also act in a synergistic manner and wanted to better understand the role of non-potent analogs. We performed a series of experiments with various combinations of different compounds isolated from extracts and purchased standards. The results indicate that less potent capsaicinoids, in general, tend to act as positive modulators and increase the overall potency of the capsaicin / capsaicinoid mixture (Fig. 4*D* and Supplementary Table 4). Non-activating compounds, namely capsaicinoids **28** and **29**, capsiate **39** and the precursor vanillin **40**, resulted in the greatest positive modulation of capsaicin induced TRPV1 activation. It was found that channel opening begins with the binding of the vanilloid head (76) and that only two ligands are needed for the receptor activation (78). According to the most recent findings, all four capsaicin binding sites play an equal stepwise role in channel activation (76, 78, 79). Based on the above, non-pungent vanilloids (i.e. capsaicinoids **28** & **29** and related vanilloids **39** & **40**) appear to collectively facilitate the transition of the TRPV1 channel due to the shared vanilloid head. Also, some weakly activating capsaicinoids, as illustrated by the curve of capsaicinoid **34** in Fig. 4D, might simply be additive to strong TRPV1 agonists (see Supplementary Table S4 for the data of all tested combinations).

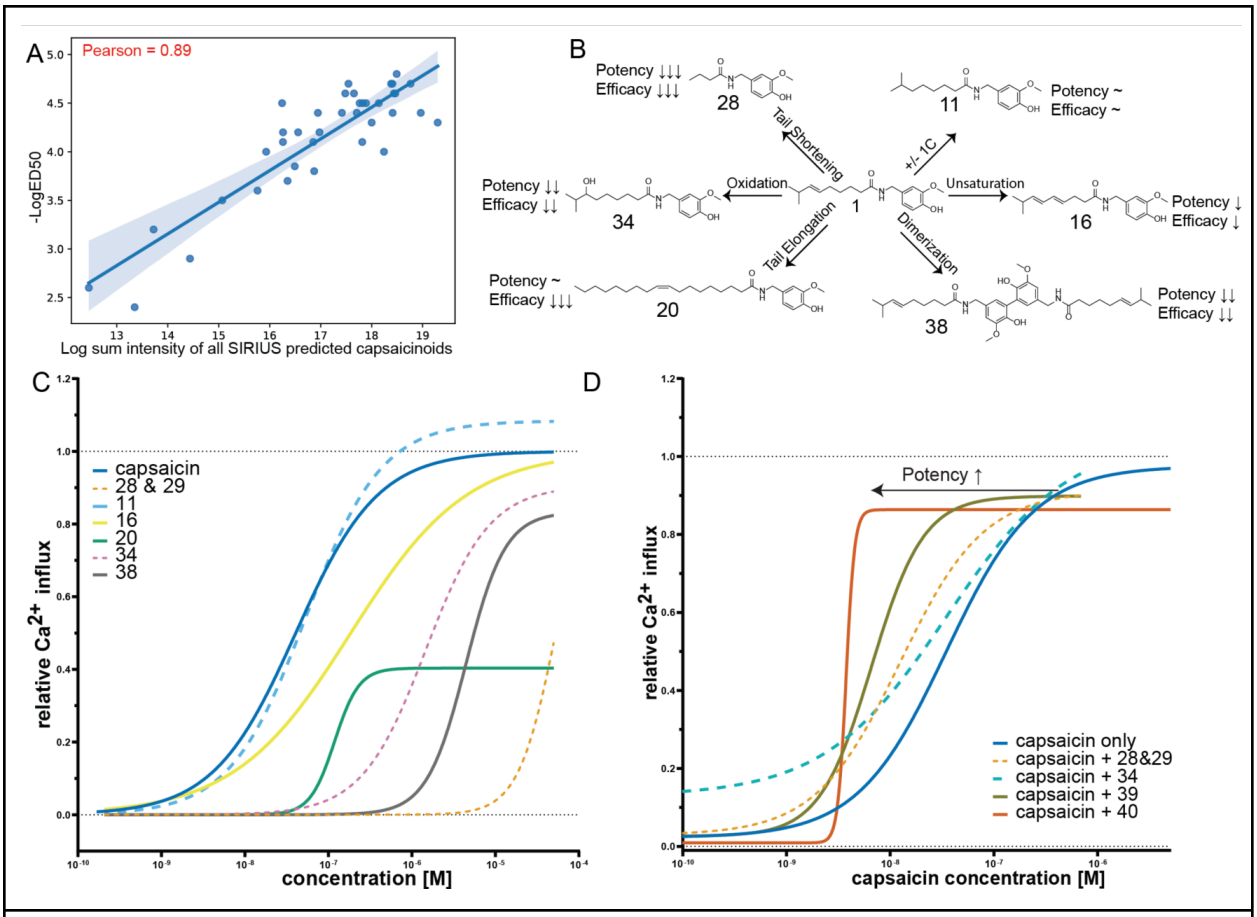

Fig. 4. Effects of chili extracts and pure capsaicinoids on rTRPV1 activation (A) Relation between total capsaicinoid content and TRPV1 activation. Each point corresponds to one chili variety. For each variety, the sum intensity of MS peak area for predicted capsaicinoids is plotted against its corresponding $-\text{LogED}_{50}$ value. S7 and S25 were removed from the data analysis, see Supplementary table 2. Removal of the two varieties did not change the overall positive trend. (B) Modifications of capsaicinoids and how they affect rTRPV1 response. Relative to capsaicin, most modifications result in decreased potency and efficacy. (C) Activation curves of capsaicinoids representative of their group. All values were normalized against that of capsaicin. (D) Capsaicin-induced rTRPV1 activation modulated by a non-potent analog or precursor. Concentrations of capsaicinoids added: **28** and **29** – 1.7 μM, **34** – 0.2 μM, **39** – 1.7 μM, **40** – 1 μM. These single concentrations were added to a dilution series representing a full dose–response curve of capsaicin. A full description of the curves for combinations of capsaicinoids is provided in Supplementary table 4.

Conclusions

In the process of exploring capsaicinoids, we have assembled the most comprehensive library of naturally occurring capsaicinoids with NMR structure confirmation. Our data show that most variations of capsaicinoid molecules reside in varying carbon tail length, sometimes with

different degrees of oxidation or reduction, in line with findings of previous studies. Some of the capsaicinoids we discovered bear modifications to their vanilloid heads. However, these compounds seem to be unstable based on repeated NMR and MS measurements, thus excluded from further testing.

Previously, it was speculated, based on targeted analysis, that capsaicinoids were of no use for chemotaxonomic identification(9). Our untargeted analysis corroborates this suspicion as the capsaicinoid fingerprints obtained did not allow for reliable species identification. Variation in the composition of capsaicinoid mixtures is important when considering chilis for use in medicinal products.

Capsaicinoid mixtures from natural chili extracts, although not species-specific, were found highly effective to gauge rTRPV1 activation. Mixtures acted synergistically and were not dependent on capsaicin or dihydrocapsaicin as the sole driving force of rTRPV1 activation. The potency of most capsaicinoids is proportional to their similarity to capsaicin. Oxidation of the tail greatly reduces the potency of capsaicinoids, so protection against oxidation is recommended for maintaining their potency. Capsaicinoids with long acyl tails have similar potency but are less efficient compared to capsaicin. Conversely, shorter-tailed capsaicinoids are progressively less active and those with a tail about two carbons long are inactive altogether. Nevertheless, despite the loss in individual potency, these capsaicinoids act together synergistically.

Additionally, non-activating compounds can function as positive modulators of capsaicin activity. The non-activating precursor vanillin, which is found in smaller concentrations in chilis, can add to the overall synergistic effect of rTRPV1 activation. Capsaicin and dihydrocapsaicin are typically the most abundant capsaicinoids, but they should not be the only compounds considered with respect to TRPV1 activation. Ultimately, all chili derived products that use normalized extracts can experience batch-to-batch variation in capsaicinoid profiles.

Limitations of this study

We selected only four species of chili with ones leaning on the spicier side. For full understanding of the chemical space, less spicy varieties and wild cultivars should be included in future studies. All capsaicin modulation and antagonism experiments began with premixing all compounds and delivering them in parallel. Experiments could also be completed with pretreatment of compounds, however, this should not change any conclusions from our results . While our data illustrated a synergism between capsaicin and non-activating related compounds and other capsaicinoids, we did not investigate the exact mechanism. Lastly, all the experiments were done on the rat, not human, TRPV1 receptor which may not translate completely despite the high homology of the two proteins.

Methods

Plant collection and sample preparation

In obtaining material for this study, we collaborated with the Botanical Garden of the Faculty of Tropical AgriSciences of the Czech University of Life Sciences in Prague. Each year the garden regrows chilis to maintain a collection of chili seeds. Chili sowing begins between January and February and continues into summer and early fall months. In cases of increased pest infestation, plants are subjected to chemical treatment with acetamiprid, a common insecticide. The botanical garden has confirmed the varieties in its collection by comparing their morphological traits with those of plants grown at other botanical gardens or by verified dealers. For our present study, we harvested ripe chilis on several occasions between the months of August and October. Ripeness was assessed based on fruit coloration (80), (Fig. S1). In total, we collected 40 different varieties covering a wide range of heat levels (Table 1). Unfortunately, at the time of collection, we were unable to obtain fruits of the species *C. pubescens*, which has been reported to have atypical capsaicinoid fingerprints, and we did not include wild chilis (9) in the scope of our study.

There, chili plants analyzed in our study were sown in winter months, from December to February, transplanted to pots throughout March and finally replanted into polycarbonate-covered flower beds or backup containers at the end of May. The chilis were grown in an ordinary horticultural substrate fertilized with cow manure. Chilis and sometimes stems were collected when ripe – based on size, shape and color – and immediately placed on dry ice. They were then stored at −80 °C until further processing, in which they were crushed to a powder with a pestle and mortar under liquid nitrogen, lyophilized and again stored at−80 °C until analysis and experimentation.

Chili extraction

Approximately 1 g of chili powder was used for extraction with 25 ml of ethyl acetate (EtOAc) and agitation provided by an IKA dispenser for 1 minute. This process was completed twice for each variety. Pooled extracts from each variety were evaporated and then subjected to acetonitrile:hexane partitioning with a ratio of 1:1. The acetonitrile portion was dissolved to 1 mg/ml in acetonitrile (ACN), spun down at high speeds. A portion of the spun-down sample was diluted to 0.2 mg/ml and analyzed by LC-MS.

First large-scale extraction. Different varieties of lyophilized chilies (see Table 1 for the specific varieties) were mixed together, about 50g. The mixed chili powder was submerged in an excess of EtOAc and stirred for two hours at room temperature. The EtOAc was decanted, filtered through Whitman No. 1 filter papers and collected into a round-bottom flask. The EtOAc was then removed under vacuum (rotary evaporator, Buchi) and reused for subsequent extractions. The remaining plant material was extracted two more times in a similar manner, but with 4 hours and then 16 hours of stirring. The extracts were pooled together. This crude extract mixture was

then fractionated by normal-phase flash chromatography on a CombiFlash Rf 200 system (Teledyne) at a flow rate of 30 ml/min. Mobile phase A: Cyclohexane. Mobile phase B: EtOAc. 0 → 45 minutes of isocratic 45% B; 45 → 75 minute gradient from 45% B to 100% B; 75 → 85 minutes 100% B. The fractions were pooled into 7 fractions based on LC–MS analysis. These pooled fractions were isolated using a 1260 Infinity II Preparative LC system (Agilent) with a 19 mm × 250 mm Waters XBridge C18 column for 65 minutes, using a Milli-Q water:eACN(Fisher) gradient. Gradients started at either 25% or 30% ACN and went to 100% ACN.

Second large-scale extraction. The second large-scale extraction followed similar procedures as the first, only with some optimization to the LC methods. EtOAc in excess was added to pooled lyophilized chili powder, about 89 g. Each sample was macerated with stirring for 1 hour and 30 minutes. The extract was then filtered into a round-bottom flask, and the EtOAc was evaporated under vacuum (rotary evaporator, Buchi). The EtOAc was then reused to extract the chili sample again. This was completed six times. On the last maceration, the sample was left overnight while stirring at room temperature. After this overnight maceration, the extract was filtered and pooled with the previous extracts. The remaining plant material was washed with a small portion of EtOAc and added to the pooled extract. The pooled extract was then filtered through Whitman No. 1 filter papers. Normal-phase flash chromatography (Teledyne) was then repeated with an optimized gradient for better peak separation. Mobile phase A: Cyclohexane. Mobile phase B: EtOAc. 0 → 8.4 minutes isocratic 10% B, 8.4 → 16.8 minutes 10% → 20% B,16.8 → 34.9 minutes isocratic 20%B, 34.9 → 36.9 minutes 20% → 40%B, 36.9 → 56.9 minutes isocratic 40%B, 56.9 → 70 minutes 40% → 100%B, 70 → 78 minutes 70 → 78 minutes. The fractions were checked by LC–MS and pooled to maintain the highest purity of the target compound. Pooled fractions were further separated by preparative HPLC (Agilent) equipped with a 10 mm × 250 mm Waters XBridge C18 column. The LC methods were optimized using an XBridge C18 3.5 μm column (Waters) and then transferred to an XBridge C18 10 mm × 250 mm (Waters) and then fine-tuned. The methods were optimized for the isolation of as many target capsaicinoids as possible.

Dereplication of capsaicinoids

We also applied our dereplication pipeline to aid in the search for novel capsaicinoids. By querying Reaxys and Wikidata, we were able to identify 25 previously reported capsaicinoids from *Capsicum*(Fig. 1). Our output from the search was greater than 25 compounds with some inconsistencies in the literature and the storage of data. Capsaicin was sometimes stored with a SMILES string indicative of a mixture of *cis* and trans isomers despite natural capsaicin existing almost exclusively in the trans form. The carbon–carbon double bond adjacent to the terminal isopropyl group is speculated to be formed by the enzyme desaturase(81). While many desaturases result in *cis* configuration, plants are known to be home of many atypical fatty acids with those in the *trans* configuration (82, 83). However, this is yet to be confirmed experimentally. We also had to contend with the known problem concerning the nomenclature of the different compounds referred to as homocapsaicin (84). To avoid confusion, we refer to the

structure/name pairs used in the original publication (11). The confusion regarding homocapsaicin is caused by the fact that homocapsaicin-II is reported as homocapsaicin in the works of Wang et. al. (41). Furthermore, many studies reporting on the structural confirmation or isolation of capsaicinoids relied solely on MS characterization without library matching or orthogonal confirmation. Although the structures themselves are still reliable for dereplication purposes, the interpretation of analytical results concerning capsaicinoids should be taken with caution, especially with suspected or known alkyl tail isomers. Lastly, two other capsaicinoids, livnvanil and myrvanil, have been suggested to be found in *Capsicum* oleoresin; however, these have never been isolated from this extract, so they were left off the list (85).

LC–MS analysis

An Orbitrap ID-X mass spectrometer (Thermo Fisher) coupled to a Vanquish Duo UHPLC system (Thermo Fisher) was used. The temperature of the column compartment was set to 40"°C. A Waters Acquity BEH C18 150„×„2.1 mm, 1.7 µM , 130 A column was used. Samples were injected in 1 µl quantities. A Waters Vion mix was injected as a separate instrument QC sample. Mobile phase A: LC–MS-grade water + 0.1% MS-grade formic acid. Mobile phase B: LC–MS-grade acetonitrile + 0.1% MS-grade formic acid. The flow rate was set to 0.350 ml/min. 0 minutes 5%B → 0.5 minutes 5%B → 15.5 minutes 100%B → 17.3 minutes 100%B → 17.3 minutes 5%B → 19.3 minutes end of run. The ion source was set to 3000 V, the gas mode was set to static, 50 sheath gas (arb), 10 aux gas (arb), 1 sweep gas (arb). The temperature of the ion transfer tube was 325°C and the vaporizer temperature was 350°C. The Orbitrap resolution was set to 60,000 with a scan range of 100–1000 m/z, the rf lens was set to 45%, and the maximum injection time was set to 118 seconds. The MS/MS was set to 0.6-second cycles, with 1.0×10^5 signal intensity triggering the MS/MS scan. Fragmented ions were added to an exclusion list with a 5 ppm tolerance for 2 seconds after initial triggering. Isotopes were also excluded. Apex detection was used with an FWHM value of 4 and a 50% window. The MS/MS isolation window was 0.8 m/z, with HCD fragmentation with a fixed energy mode at 35%. MS/MS detection took place in the orbitrap, with a resolution of 15,000 and 80 ms maximum injection time.

Untargeted metabolomics data processing

Thermo Fisher .raw files obtained from the UPLC–MS run were converted to .mzML files using MSconvert. The MSconvert settings were set to values recommended in MZmine documentation (86). The converted files were then processed using MZmine version 4.0.8 (6, 33). Processed MZmine data and the corresponding feature table was exported to .mgf files using both the SIRIUS and GNPS export routines. MZmine parameters can be found in the corresponding batch file and as follows. Mass detection was performed for centroided MS and MS/MS signals separately, with 'Noise Levels' set to 1.0×10^4 and 1.0×10^3 signal intensity, respectively. Chromatogram building was carried out using the ADAP Chromatogram Builder Module, using the following parameters: a minimum of 6 consecutive scans, a minimum group intensity of 5.0×10^4, a minimum absolute height of 1.0×10^5 and m/z tolerance for scan-to-scan

matching of 0.001 m/z or 3.5 ppm. Chromatograms were smoothed using the Savitzky–Golay filter with retention time smoothing and 5 points. A local minimum resolver was used for feature deconvolution, with the following parameters: retention time dimension, a chromatographic threshold of 0.95%, a minimum search range of 0.05 (retention time or mobility), 5.0% minimum relative height, a minimum peak height of $1.0x10^5$, a minimum ratio of peak top/edge of 3.00, a peak duration of 0–2 and a minimum of 6 scans. 'MS/MS scan pairing' was also checked in the deconvolution step using the following parameters: MS1 to MS2 precursor tolerance of 0.0020 or 5 ppm, feature edges as a retention time filter, 25.0 as a minimum relative feature height, 1 minimum required signal and 1% minimum signal intensity. Isotopic patterns were grouped using the ^{13}C isotope filter. The grouping was conducted with a 0.001 m/z tolerance or 2 ppm and a retention time tolerance of 0.03 minutes. A monotonic shape constraint was applied, with the most intense isotope selected as the representative one. Other isotopic peaks were identified: 0.0010 m/z or 2 ppm tolerance, maximum charge of isotope m/z to 1 and search for single most intense scans. Join aligner was utilized to align detected features across samples: alignment was performed with an m/z tolerance of 0.010 or 3.50ppm and a retention time tolerance of 0.07 min, m/z and RT weights were set to 1. Duplicate peak filter was set to new average mode, 0.0010 m/z and 3.0 ppm tolerance and a 0.01 retention time tolerance. Feature list blank subtraction required 1 detection in blank, based on peak area with maximum ratio type and features only above a 300%-fold change were kept. Correlated features were determined with 0.01 RT tolerance, 0 and 0 were used for minimum feature height and intensity. A minimum of 1 sample was required with 60% overlap and all gap-filled features were excluded. 6 points, with 3 points on edge were required for feature shape correlation, which was based on Pearson and required 85%. Adducts were identified with ion identity networking using 0.0010 m/z or 3 ppm mass tolerance and a 0 height. Smaller networks without major ion, delete smaller networks: link threshold (set to 4) and delete networks without monomer were all enabled. Ions used were: [M]+, [M+H]+, [M+NH4]+,[M+Na]+,[M+K]+,[M+2H]2+,and [M-H20}]. An additional ion was manually added to the MZmine list, [M+ethylamine]+ (46.0651). Feature lists were filtered by rows requiring 1 isotope feature, MS/MS scan and feature IDs were reset. Features were then matched with the capsaicinoid library using merged MS/MS spectra, precursor tolerance of 0.0010 or 5 ppm, spectral tolerance of 0.0015 m/z or 10 ppm, removed precursor, minimum of 5 matched signals, weighted cosine similarity based on MassBank and a minimum score of 0.8, all unmatched signals were kept and matched to zero.

Exported .mgf files were then uploaded to GNPS library (40 varieties : ID=109485b44f8b437caf0db5ffe480e7af and Large-scale extraction: ID=ffca33c3005c4251b8bc9e064f383fa8). The GNPS precursor and fragment mass tolerance was set to 0.0075 Da. Minimum cosine pairing was set to 0.65, with 5 minimum matched fragments, 500 Da maximum shift in precursor. Network TopK was set to 15 and the component size was 150. All other parameters were set to their default values. For SIRIUS, version 4.13.3, the mass analyzer parameter was changed to 'orbitrap', the 'bio databases' option was selected, and values greater than 800 Da were excluded from the analysis; all other SIRIUS parameters were kept at their default values. All exports from SIRIUS, GNPS and MZmine were post-processed using Python scripts for database dereplication and merging export tables with needed information for eventual Cytoscape overlay. The Python scripts can be found at

https://github.com/jdsmith145/Capsaicinoids. All raw and processed data files and MSconvert batch files, detailing the MSconvert settings used, are deposited in the MassIVE repository under reference number MSV000096223 or at 10.5281/zenodo.13987764 .

UV and CD

The concentrations of isolated capsaicinoids used for testing were measured using a Thermo Fisher Nanodrop spectrophotometer. DMSO was used as a blank. ECD and absorption spectra were measured on a Jasco 1500 spectrometer over a spectral range of 180 nm to 350 nm in dACN (1.5 mM solutions). Measurements were made in a cylindrical quartz cell with a 0.02 cm path length, using a scanning speed of 10 nm/min, a response time of 8 seconds, standard instrument sensitivity and 3 accumulations. After a baseline correction, the resulting spectra were expressed in terms of differential molar extinction ($\Delta\varepsilon$) and molar extinction (ε), respectively.

NMR

NMR spectra were measured on a 500 or a 600 MHz Bruker Avance III HD spectrometer (^{1}H at 500.0 or 600.1 MHz and ^{13}C at 125.7 or 150.9 MHz) in CD_3CN or DMSO-d_6. The spectra were referenced to solvent signals (CD_3CN: δ = 1.94 and 1.32 ppm for ^{1}H and ^{13}C, respectively; DMSO-d_6: δ = 2.50 and 39.52 ppm for ^{1}H and ^{13}C, respectively). The signal assignment was performed using a combination of a 1D (^{1}H and ^{13}C) experiment and 2D correlation experiments (H,H-COSY, H,C-HSQC and H,C-HMBC). In some cases, the sample quantity was insufficient for the detection of some or all ^{13}C signals in the 1D experiments. The structural analysis and signal assignment was then based on the 2D correlation experiments. All NMR data was deposited to NP-MRD; all ID's for individual compounds can be found in Supplementary File 2.

Inducible TRPV1 Cell Line

The full-length open reading frame for rat TRPV1 was amplified by PCR in a Veriti thermal cycler (Applied Biosystems, Thermo Fisher Scientific, MA, USA) from pcDNA3-rTRPV1-N604S (generously provided from Rachel Gaudet), using gene-specific oligonucleotide primers encompassing AsiSI and MluI restriction sites (Table 1) and Advantage Polymerase mix (Takara Bio, USA). The AsiSI-MluI-digested rTRPV1 DNA fragment was ligated into the pcDNA™5/FRT/TO plasmid (Invitrogen, Thermo Fisher Scientific) modified to contain AsiSI/MluI cloning sites, and transformed into Stbl3 *E. coli* cells, prior to plasmid DNA purification and Sanger sequencing verification. The final pFRT-TO-rTRPV1-FLAG construct was preceded by a cytomegalovirus (CMV) promoter containing a tetracycline-controlled transcriptional repressor (2

× 19-bp $TetO_2$) sequence. Downstream of the ORF, the final expression cassette was engineered to contain a Ser-Gly (AGTGGA) peptide linker followed by a FLAG-epitope sequence (ATTACAAGGATGACGACGATAAGGTT) and a stop codon.

Flp-In T-REx-293 parental cells containing a single integrated Flp Recombination Target (FRT) site (Invitrogen) were cultured in a HERAcell 150i CO_2 incubator at 37 °C (Thermo Scientific) in a 10-cm tissue culture dish (VWR, Radnor, PA, USA) in Advanced Dulbecco's Modified Eagle Medium (Adv-DMEM/F12) (Life Technologies, Inc.) supplemented with 10% fetal bovine serum (FBS, Gibco), 16 µg/mL Blasticidin (Life Technologies, Inc) and 100 µg/mL Zeocin (Life Technologies, Inc). Flp-In™ T-REx-293™ were seeded in a 6-well tissue culture dish (VWR) at a density of 0.3 x 10^6 cells in 1.5 mL Adv-DMEM/FBS without antibiotics. After 48 hrs, cells in three separate wells were co-transfected (day 0) with 4.5 µg endotoxin-free pOG44, 1 µg endotoxin-free rTRPV1-FLAG plasmid DNAs and 10 µL Lipofectamine (L2000, Invitrogen) diluted in 300 µL Opti-MEM I Reduced Serum (Life Technologies). The next day (day 1) the transfection medium was gently decanted and replaced with 2 mL Adv-DMEM/FBS for 48 hrs.

On day 3 post transfection, cells from each transfection were trypsinated using 0.5 mL Trypsin-EDTA 1X 0.25% (Corning, Corning, NY, USA) and replated in a 6-cm culture dish in 5mL Adv-DMEM/FBS and 200 µg/mL Hygromycin B (Life Technologies) to start selecting for transformants. The selection medium was decanted on day 5, day 8 and day 12 post transfection and replaced with fresh Adv-DMEM/FBS and 200 µg/mL Hygromycin, for a total of 3 changes. Single-cell transformants observed on the experimental transfections plates were allowed to expand for an additional 5 days, after which lines containing individual Flp-In T-REx transformant colonies were established in presence of Hygromycin and Blasticidin. Final monoclonal lines (irTRPV1-FlpIn293) were validated via qPCR and western blot after induction for 48h with Doxycycline 1 mg/mL .

TRPV1 activity assay

A stably transfected irTRPV1-FlpIn293 cell line using a Tet-on system was created as described above. Cells were grown to confluence in Adv-DMEM/F12 supplemented with 10% FBS, 1% Pen Strep, 1% Glutamax (all Gibco, Thermo Fisher Scientific). 48 hours before the experiment, doxycycline (final concentration 1 µg/mL) and 10 µM ruthenium red (RR) was added to the media to induce TRPV1 expression. After 24 hours, the cells were washed and detached with 0,5% trypsin–EDTA in PBS (Gibco). Cells resuspended in blocking media (Adv-DMEM/F12 + 10% FBS + 10 µM RR) were counted and then seeded into a 384 well plate (3674, Corning) in amount 30 k/well. 24 hours after seeding 2X Fluo-4 direct dye solution (Invitrogen), dissolved in HHBS buffer, pH ~ 7.4; was added to well with cells and incubated 30 minutes at 37°C and then for 40 minutes at room temperature. Once incubated with dye, supernatant was removed using BlueWasher (BlueCatbio NH Inc., Lebanon, NH, USA) and changed to HHBS+ 10 µM

sulfinpyrazone (pH ~ 7.4) solution added by Certus (Fritz Gyger AG, Gwatt, Schwitzerland), followed by 10 minutes of incubation in FDSS µCell (~ 30°C; Hamamatsu, Hamamatsu city, Japan). A separate compound plate was prepared using an Echo dispenser (Beckman Coulter Inc.,Brea, CA, USA). The final concentration was reached by adding the HHBS + 10 µM sulfinpyrazone as above by Certus. The rTRPV1 activity measurement started by recording the baseline (40 s, sample interval 0.339 s). Then the compounds were transferred to the dedicated wells by tips while the recording was running for next 5 minutes. The 1% TritonX-100 and 1 µM capsaicin were used for normalization of the data by an internal laboratory management system ScreenX (version 2.0, developed at Institute of Molecular Genetics, Prague, Czechia) and GraphPad Prism (version 10.2.2 (397), GraphPad Software). All dose-response curves were done as least square fit with separately handled replicates.

Acknowledgments

J.D.S. was supported by the Charles University Grant Agency (GA UK) and the First Faculty of Medicine of Charles University, project ID: 252182 376322 Smith. T.P. was supported by the Czech Science Foundation (GA CR) grant 21-11563M and by the European Union's Horizon 2020 research and innovation programme under Marie Skłodowska-Curie grant agreement No. 891397. V.T.S. was supported by the Ministry of education and health of the Czech republic (LM2023052). We want to greatly thank The Botanical Garden of the Faculty of Tropical AgriSciences of the Czech University of Life Sciences Prague (CZU) for donation of the chilis and the continuous collaboration. A special thanks to the Pluskal Group, Teo Hebra for the continuous support, and Roman Bushuiev for help with Python scripts. Lastly, we want to thank Frederick Rooks for the comprehensive edits and suggestions to the manuscript.

Supplementary data

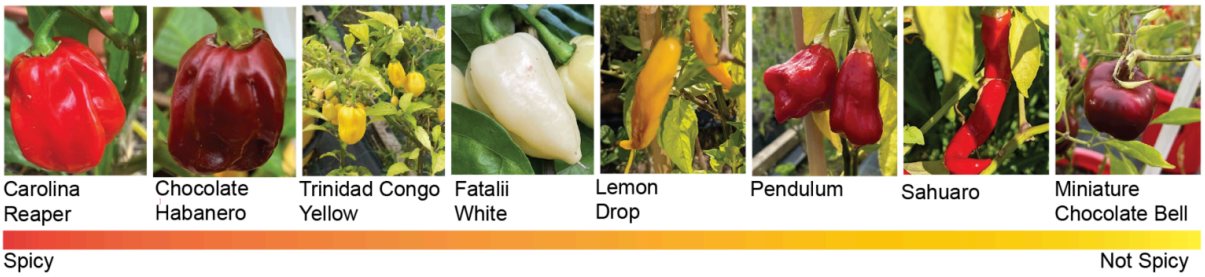

Fig. S1. Example photos of chili that were collected and extracted

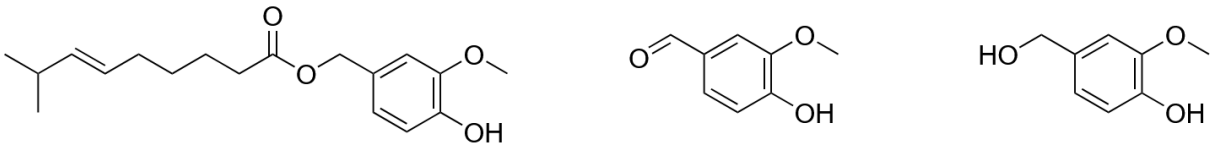

39 40 41

Fig. S2. Three compounds used in rTRPV1 testing but are not capsaicinoids. **39** is capsiate, **40** is vanillin and **41** is vanillyl alcohol.

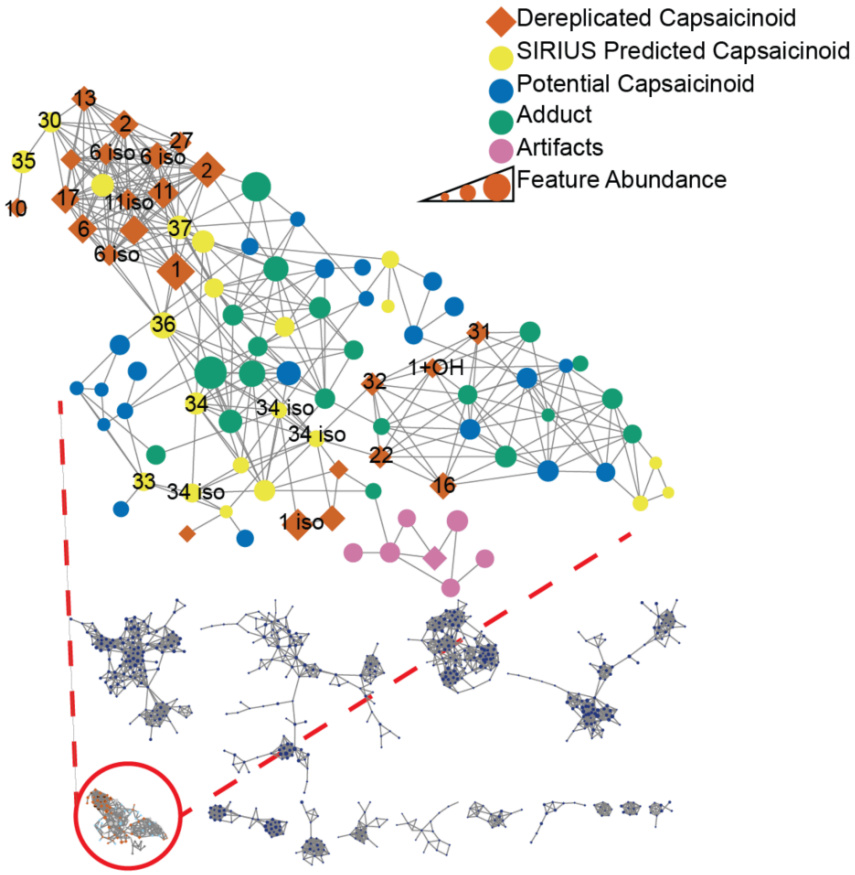

Fig. S3. Unprocessed network from the initial 40 chili extractions. Potential capsaicinoids are features indicative of a structure similar to a vanilloid head based on MS/MS spectra but were not identified as capsaicinoids by SIRIUS. Adducts are ions of repeated nodes with different counter ions, e.g. [M+H]+, [M+Na],[M+ethylamine]+ and [2M+H]+. Artifacts are features unrelated to capsaicinoids but were clustered there as a result of the networking process.

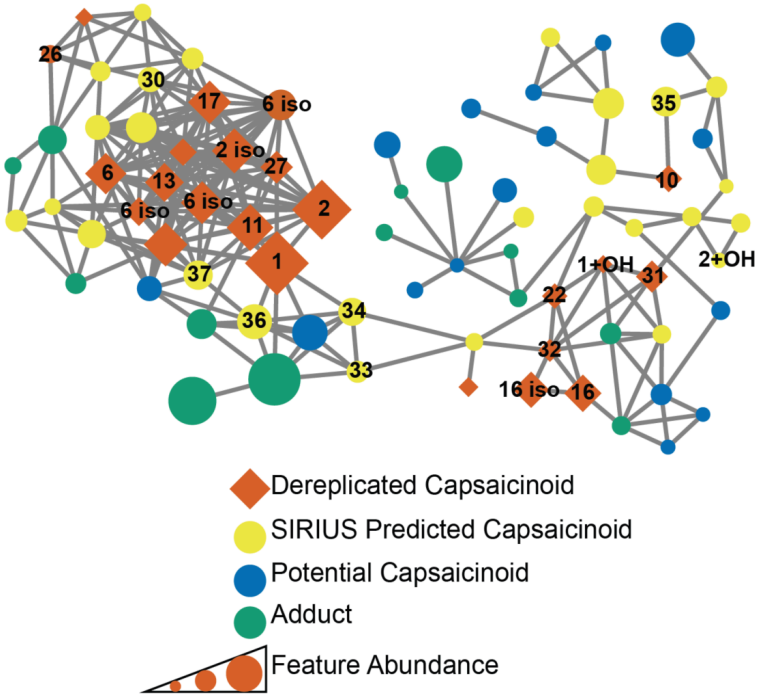

Fig. S4. Unprocessed network from the large-scale chili extraction. Potential capsaicinoids are features indicative of a structure similar to a vanilloid head based on MS/MS spectra but were not identified as capsaicinoids by SIRIUS. Adducts are ions of repeated nodes with different counter ions, e.g. [M+H]+, [M+Na],[M+ethylamine]+ and [2M+H]+.

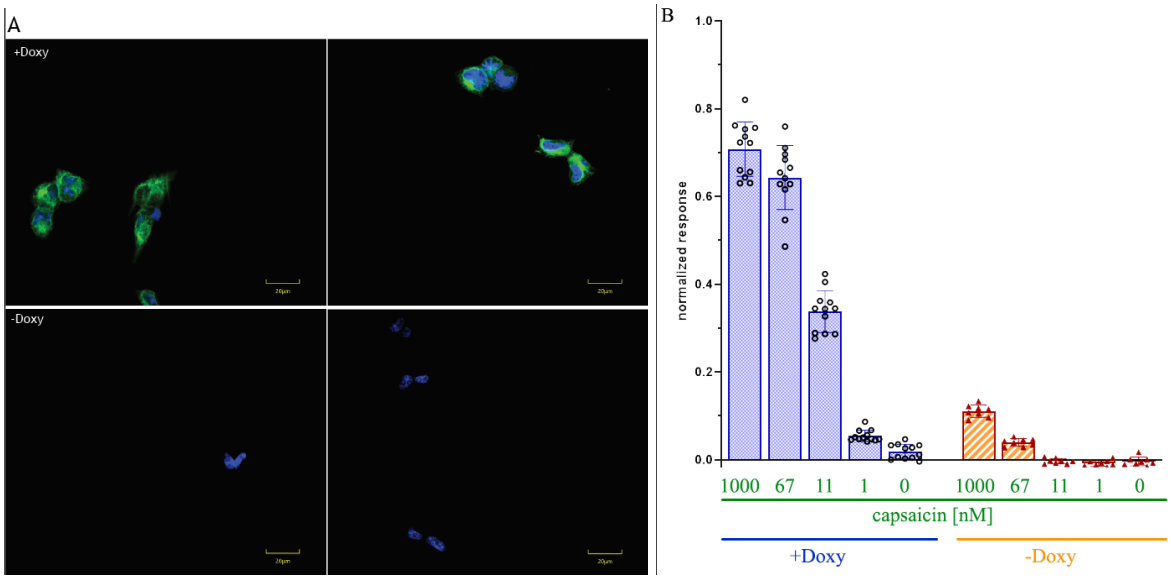

Fig. S5. Comparison of irTRPV1-FlpIn293 cell-line with and without induction by doxycycline (Doxy) . (a) Immunocytochemical staining of irTRPV1-FlpIn293+Doxy (top row) and -Doxy (bottom row). Nucleus (blue; DAPI), rTRPV1 receptor (green; sc-398417 (1:200, 1 hour, RT) + ab150115 (1:800, 1 hour, RT)). Recorded by Yokogawa CV8000, 60x objective. The non-induced cells alone express an enhanced number of receptors, which is not obvious from figures, because the gain was adjusted to the induced (+Doxy) cells with an excessive number of receptors. (b) Calcium influx after application of capsaicin to the induced (+Doxy, blue) and non-induced cells (-Doxy, orange), according to protocol described in Methods. The peak values are normalized to 1% TritonX-100.

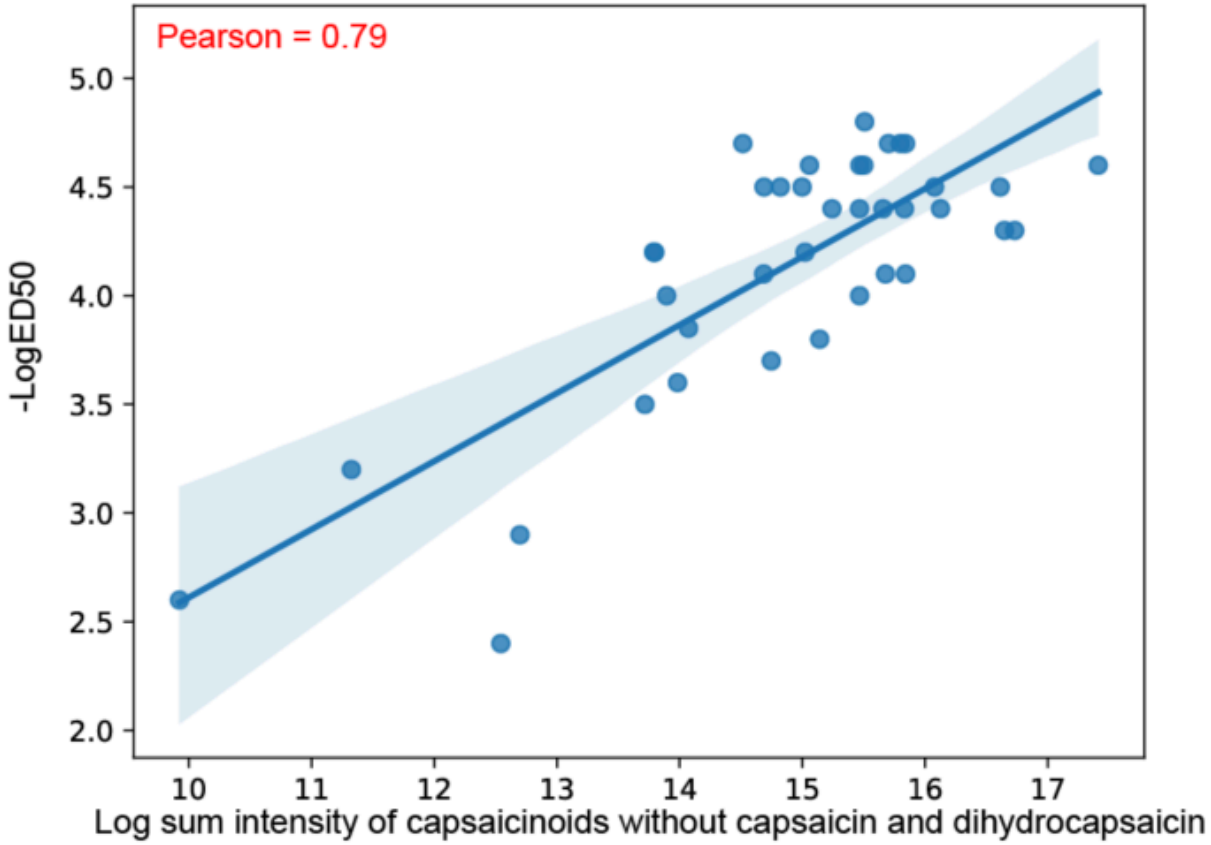

Fig. S6. Comparison of sum intensities of all predicted capsaicinoids excluding capsaicin and dihydrocapsaicin and its activity on rTRPV1. [M+H]+, [M+Na],[M+ethylamine]+ and [2M+H]+ adducts were removed for both capsaicin and dihydrocapsaicin. Black Prince (S7) and Miniature Chocolate Bell (S25) were not plotted. A strong correlation persists even without capsaicin and dihydrocapsaicin.

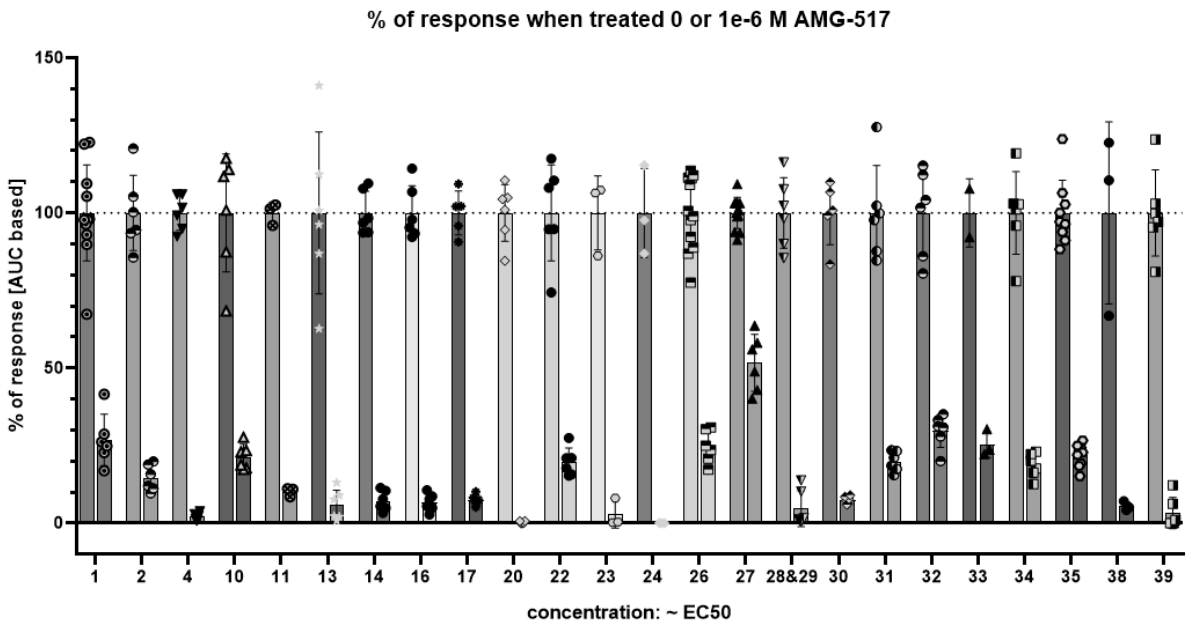

Fig. S7. Compounds were added in a concentration close to their EC_{50} along with 1,7 μM AMG-517 or without to determine inhibition. The area under the peak was used for evaluation of the inhibition. Some compounds showed greater inhibition than others. Since capsaicinoid and inhibitor were added simultaneously, it is possible that the compound was out competed in different manner.This can reflect different binding modes of the capsaicinoids.

1. F. Liu, *et al.*, Genomes of cultivated and wild Capsicum species provide insights into pepper domestication and population differentiation. *Nat. Commun.* **14**, 5487 (2023).

2. S. Atwal, Pepper X dethrones Carolina Reaper as world's hottest chilli pepper. *Guinness World Records* (2024). Available at: https://www.guinnessworldrecords.com/news/2023/10/pepper-x-dethrones-carolina-reaper-as-worlds-hottest-chilli-pepper-759706 [Accessed 16 October 2023].

3. W. L. Scoville, Note on capsicums. *J. Am. Pharm. Assoc. (1912)* **1**, 453–454 (1912).

4. J. E. Woodbury, Determination of Capsicum pungency by high pressure liquid chromatography and spectrofluorometric detection. *Journal of the Association of Official Analytical Chemists* **63**, 556–558 (1980).

5. How Do You Measure the "Heat" of a Pepper? *How Do You Measure it?* (2022). Available at: https://www.nist.gov/how-do-you-measure-it/how-do-you-measure-heat-pepper [Accessed 1 June 2024].

6. R. Schmid, *et al.*, Integrative analysis of multimodal mass spectrometry data in MZmine 3. *Nat. Biotechnol.* **41**, 447–449 (2023).

7. L.-F. Nothias, *et al.*, Feature-based molecular networking in the GNPS analysis environment. *Nat. Methods* **17**, 905–908 (2020).

8. K. Dührkop, *et al.*, SIRIUS 4: a rapid tool for turning tandem mass spectra into metabolite structure information. *Nat. Methods* **16**, 299–302 (2019).

9. Y. Zewdie, P. W. Bosland, Capsaicinoid profiles are not good chemotaxonomic indicators for Capsicum species. *Biochem. Syst. Ecol.* **29**, 161–169 (2001).

10. U. Z. Ishimov, Z. F. Ziyavitdinov, N. Z. Sagdiev, Minor constituents of total capsaicinoids from Capsicum annuum. *Chem. Nat. Compo.* **46**, 1006–1007 (2011).

11. J. Jurenitsch, M. David, F. Heresch, W. Kubelka, Nachweis und Identifizierung neuer Scharfstoffe in Capsicum–Früchten. *Planta Med.* **36**, 61–67 (1979).

12. M. D. Wilkinson, *et al.*, The FAIR Guiding Principles for scientific data management and stewardship. *Sci. Data* **3**, 160018 (2016).

13. A. L. Kurian, A. N. Starks, HPLC analysis of capsaicinoids extracted from whole orange habanero chili peppers. *J. Food Sci.* **67**, 956–962 (2002).

14. V. K. Attuquayefio, K. A. Buckle, Rapid sample preparation method for HPLC analysis of capsaicinoids in capsicum fruits and oleoresins. *J. Agric. Food Chem.* **35**, 777–779 (1987).

15. T. Stipcovich, G. F. Barbero, M. Ferreiro-González, M. Palma, C. G. Barroso, Fast analysis of capsaicinoids in Naga Jolokia extracts (Capsicum chinense) by high-performance liquid chromatography using fused core columns. *Food Chem.* **239**, 217–224 (2018).

16. Impact of Sex in the Effect of Dietary Capsaicin on Cardiovascular Health. *clinicaltrials.gov* (2024). Available at: https://clinicaltrials.gov/study/NCT06363305 [Accessed 25 October 2024].

17. Capsimax Effect on Metabolic Rate, Satiety and Food Intake. *clinicaltrials.gov* (2018). Available at: https://clinicaltrials.gov/study/NCT03489226 [Accessed 25 October 2024].

18. M. J. Caterina, *et al.*, The capsaicin receptor: a heat-activated ion channel in the pain pathway. *Nature* **389**, 816–824 (1997).

19. E. Cao, M. Liao, Y. Cheng, D. Julius, TRPV1 structures in distinct conformations reveal activation mechanisms. *Nature* **504**, 113–118 (2013).

20. C. Bae, *et al.*, Surface characterization and membrane interaction of double-knot toxin, an activator of TRPV1 channels. *Biophys. J.* **108**, 36a (2015).

21. F. Yang, *et al.*, Structural mechanism underlying capsaicin binding and activation of the TRPV1 ion channel. *Nat. Chem. Biol.* **11**, 518–524 (2015).

22. Y. Dong, *et al.*, A distinct structural mechanism underlies TRPV1 activation by piperine. *Biochem. Biophys. Res. Commun.* **516**, 365–372 (2019).

23. Y. Chu, B. E. Cohen, H.-H. Chuang, A single TRPV1 amino acid controls species sensitivity to capsaicin. *Sci. Rep.* **10**, 8038 (2020).

24. M. J. Caterina, D. Julius, The vanilloid receptor: a molecular gateway to the pain pathway. *Annu. Rev. Neurosci.* **24**, 487–517 (2001).

25. A. Patapoutian, A. M. Peier, G. M. Story, V. Viswanath, ThermoTRP channels and beyond: mechanisms of temperature sensation. *Nat. Rev. Neurosci.* **4**, 529–539 (2003).

26. K. Elokely, *et al.*, Understanding TRPV1 activation by ligands: Insights from the binding modes of capsaicin and

resiniferatoxin. *Proc. Natl. Acad. Sci. U. S. A.* **113**, E137–45 (2016).

27. V. G. Uarrota, M. Maraschin, Â. de F. M. de Bairros, R. Pedreschi, Factors affecting the capsaicinoid profile of hot peppers and biological activity of their non-pungent analogs (Capsinoids) present in sweet peppers. *Crit. Rev. Food Sci. Nutr.* **61**, 649–665 (2021).

28. C. A. Reilly, D. J. Crouch, G. S. Yost, Quantitative analysis of capsaicinoids in fresh peppers, oleoresin capsicum and pepper spray products. *J. Forensic Sci.* **46**, 502–509 (2001).

29. T. Wu, *et al.*, Rapid Determination of Capsaicin and Dihydrocapsaicin in Fermented Pepper Paste by Direct Analysis in Real Time Mass Spectrometry. *Food Anal. Methods* **12**, 32–40 (2019).

30. N. Kozukue, *et al.*, Analysis of Eight Capsaicinoids in Peppers and Pepper-Containing Foods by High-Performance Liquid Chromatography and Liquid Chromatography−Mass Spectrometry. *J. Agric. Food Chem.* **53**, 9172–9181 (2005).

31. A. Peña-Alvarez, E. Ramírez-Maya, L. A. Alvarado-Suárez, Analysis of capsaicin and dihydrocapsaicin in peppers and pepper sauces by solid phase microextraction-gas chromatography-mass spectrometry. *J. Chromatogr. A* **1216**, 2843–2847 (2009).

32. M. Sganzerla, J. P. Coutinho, A. M. T. de Melo, H. T. Godoy, Fast method for capsaicinoids analysis from Capsicum chinense fruits. *Food Res. Int.* **64**, 718–725 (2014).

33. S. Heuckeroth, *et al.*, Reproducible mass spectrometry data processing and compound annotation in MZmine 3. *Nat. Protoc.* 1–45 (2024).

34. K. Dührkop, *et al.*, Systematic classification of unknown metabolites using high-resolution fragmentation mass spectra. *Nat. Biotechnol.* **39**, 462–471 (2020).

35. M. Ludwig, M. Fleischauer, K. Dührkop, M. A. Hoffmann, S. Böcker, De Novo Molecular Formula Annotation and Structure Elucidation Using SIRIUS 4. *Methods Mol. Biol.* **2104**, 185–207 (2020).

36. K. Ogawa, *et al.*, Evidence of capsaicin synthase activity of the Pun1-encoded protein and its role as a determinant of capsaicinoid accumulation in pepper. *BMC Plant Biol.* **15**, 93 (2015).

37. K. Kobata, T. Todo, S. Yazawa, K. Iwai, T. Watanabe, Novel Capsaicinoid-like Substances, Capsiate and Dihydrocapsiate, from the Fruits of a Nonpungent Cultivar, CH-19 Sweet, of Pepper (Capsicum annuum L.). *J. Agric. Food Chem.* **46**, 1695–1697 (1998).

38. K. Sano, *et al.*, Vanillin reduction in the biosynthetic pathway of capsiate, a non-pungent component of Capsicum fruits, is catalyzed by cinnamyl alcohol dehydrogenase. *Sci. Rep.* **12**, 12384 (2022).

39. Y. Lang, *et al.*, Functional loss of pAMT results in biosynthesis of capsinoids, capsaicinoid analogs, in Capsicum annuum cv. CH-19 Sweet. *Plant J.* **59**, 953–961 (2009).

40. P. M. Gannett, *et al.*, Capsaicinoids: their separation, synthesis, and mutagenicity. *J. Org. Chem.* **53**, 1064–1071 (1988).

41. R. Wang, *et al.*, Capsaicinoids from hot pepper (Capsicum annuum L.) and their phytotoxic effect on seedling growth of lettuce (Lactuca sativa L.). *Nat. Prod. Res.* **34**, 1597–1601 (2020).

42. E. K. Nelson, VANILLYL-ACYL AMIDES. *J. Am. Chem. Soc.* **41**, 2121–2130 (1919).

43. I. Ježo, Synthese des Capsaicins und einiger seiner Modellderivate. *Chem. zvesti* **29**, 714–718 (1975).

44. M. Takahashi, K. Osawa, J. Ueda, K. Okada, Anodic Synthesis of Acid Parts in Capsaicinoids and Spectroscopic Analysis. II. *PHARMACEUTICAL SOCIETY OF JAPAN* **96**, 1000–1004 (1976).

45. G. V. Buitimea-Cantúa, J. M. Velez-Haro, N. E. Buitimea-Cantúa, J. Molina-Torres, E. C. Rosas-Burgos, GC-EIMS analysis, antifungal and anti-aflatoxigenic activity of Capsicum chinense and Piper nigrum fruits and their bioactive compounds capsaicin and piperine upon Aspergillus parasiticus. *Nat. Prod. Res.* **34**, 1452–1455 (2020).

46. K. G. Sweat, J. Broatch, C. Borror, K. Hagan, T. M. Cahill, Variability in capsaicinoid content and Scoville heat ratings of commercially grown Jalapeño, Habanero and Bhut Jolokia peppers. *Food Chem.* **210**, 606–612 (2016).

47. C. A. Reilly, *et al.*, Metabolism of capsaicin by cytochrome P450 produces novel dehydrogenated metabolites and decreases cytotoxicity to lung and liver cells. *Chem. Res. Toxicol.* **16**, 336–349 (2003).

48. T. Ochi, Y. Takaishi, K. Kogure, I. Yamauti, Antioxidant activity of a new capsaicin derivative from Capsicum annuum. *J. Nat. Prod.* **66**, 1094–1096 (2003).

49. Y. Deng, *et al.*, Microbial transformation of capsaicin by several human intestinal fungi and their inhibitory effects against lysine-specific demethylase 1. *Phytochemistry* **202**, 113365 (2022).

50. M. Halme, *et al.*, Comparison of in vitro metabolism and cytotoxicity of capsaicin and dihydrocapsaicin. *J. Chromatogr. B Analyt. Technol. Biomed. Life Sci.* **1009-1010**, 17–24 (2016).

51. A. K. Migglautsch, *et al.*, Aliphatic hydroxylation and epoxidation of capsaicin by cytochrome P450 CYP505X. *Tetrahedron* **74**, 6199–6204 (2018).

52. B. Ma, *et al.*, Hydroxylation, Epoxidation, and Dehydrogenation of Capsaicin by a Microbial Promiscuous Cytochrome

P450 105D7. *Chem. Biodivers.* **18**, e2000910 (2021).

53. X.-L. Xin, Y. Wang, G.-J. Fan, L. Chen, C.-P. Sun, Biotransformation of capsaicin by Penicillium janthinellum AS 3.510. *Phytochem. Lett.* **19**, 210–214 (2017).

54. H. Tateba, S. Mihara, Photochemical Oxidative Dimerization of Capsaicin in an Aqueous Solution. *Agric. Biol. Chem.* **55**, 873–874 (1991).

55. M. A. Bernal, A. R. Barceló, 5,5'-Dicapsaicin, 4'-O-5-Dicapsaicin Ether, and Dehydrogenation Polymers with High Molecular Weights Are the Main Products of the Oxidation of Capsaicin by Peroxidase from Hot Pepper. *J. Agric. Food Chem.* **44**, 3085–3089 (1996).

56. D. E. Henderson, A. M. Slickman, S. K. Henderson, Quantitative HPLC Determination of the Antioxidant Activity of Capsaicin on the Formation of Lipid Hydroperoxides of Linoleic Acid: A Comparative Study against BHT and Melatonin. *J. Agric. Food Chem.* **47**, 2563–2570 (1999).

57. C. A. Reilly, *et al.*, Reactive intermediates produced from the metabolism of the vanilloid ring of capsaicinoids by p450 enzymes. *Chem. Res. Toxicol.* **26**, 55–66 (2013).

58. K. Tian, J. Zhu, M. Li, X. Qiu, Capsaicin is efficiently transformed by multiple cytochrome P450s from Capsicum fruit-feeding Helicoverpa armigera. *Pestic. Biochem. Physiol.* **156**, 145–151 (2019).

59. V. M. Martínez-Juárez, *et al.*, Specific synthesis of 5,5'-dicapsaicin by cell suspension cultures of capsicum annuum var. annuum (chili Jalapeño chigol) and their soluble and NaCl-extracted cell wall protein fractions. *J. Agric. Food Chem.* **52**, 972–979 (2004).

60. F. Saito, P. R. Schreiner, Determination of the absolute configurations of chiral alkanes – an analysis of the available tools. *European J. Org. Chem.* **2020**, 6328–6339 (2020).

61. A. Neuberger, *et al.*, Human TRPV1 structure and inhibition by the analgesic SB-366791. *Nat. Commun.* **14**, 1–10 (2023).

62. P. McIntyre, *et al.*, Pharmacological differences between the human and rat vanilloid receptor 1 (VR1). *Br. J. Pharmacol.* **132**, 1084–1094 (2001).

63. J. Lee, *et al.*, N-(3-Acyloxy-2-benzylpropyl)-N'-[4-(methylsulfonylamino)benzyl]thiourea Analogues: Novel Potent and High Affinity Antagonists and Partial Antagonists of the Vanilloid Receptor. *J. Med. Chem.* **46**, 3116–3126 (2003).

64. C. S. Walpole, *et al.*, Similarities and differences in the structure-activity relationships of capsaicin and resiniferatoxin analogues. *J. Med. Chem.* **39**, 2939–2952 (1996).

65. S. Vu, V. Singh, H. Wulff, V. Yarov-Yarovoy, J. Zheng, New capsaicin analogs as molecular rulers to define the permissive conformation of the mouse TRPV1 ligand-binding pocket. *Elife* **9**, e62039 (2020).

66. F. N. McNamara, A. Randall, M. J. Gunthorpe, Effects of piperine, the pungent component of black pepper, at the human vanilloid receptor (TRPV1). *Br. J. Pharmacol.* **144**, 781–790 (2005).

67. V. N. Dedov, *et al.*, Gingerols: a novel class of vanilloid receptor (VR1) agonists: Gingerols: a novel class of VR1 agonists. *Br. J. Pharmacol.* **137**, 793–798 (2002).

68. H. Ryu, *et al.*, Stereospecific high-affinity TRPV1 antagonists: chiral N-(2-benzyl-3-pivaloyloxypropyl) 2-[4-(methylsulfonylamino)phenyl]propionamide analogues. *J. Med. Chem.* **51**, 57–67 (2008).

69. H.-G. Park, *et al.*, N-4-methansulfonamidobenzyl-N'-2-substituted-4-tert-butyl-benzyl thioureas as potent vanilloid receptor antagonistic ligands. *Bioorg. Med. Chem. Lett.* **14**, 1693–1696 (2004).

70. J. Lee, *et al.*, Analysis of structure-activity relationships for the "B-region" of N-(3-acyloxy-2-benzylpropyl)-N(')-[4-(methylsulfonylamino)benzyl]thiourea analogues as vanilloid receptor antagonists: discovery of an N-hydroxythiourea analogue with potent analgesic activity. *Bioorg. Med. Chem. Lett.* **14**, 2291–2297 (2004).

71. C. S. J. Walpole, *et al.*, Analogs of capsaicin with agonist activity as novel analgesic agents; structure-activity studies. 3. The hydrophobic side-chain "C-region." *J. Med. Chem.* **36**, 2381–2389 (1993).

72. Y. Cho, *et al.*, The SAR analysis of TRPV1 agonists with the α-methylated B-region. *Bioorg. Med. Chem. Lett.* **22**, 5227–5231 (2012).

73. M. E. McDonnell, S. P. Zhang, A. E. Dubin, S. L. Dax, Synthesis and in vitro evaluation of a novel iodinated resiniferatoxin derivative that is an agonist at the human vanilloid VR1 receptor. *Bioorg. Med. Chem. Lett.* **12**, 1189–1192 (2002).

74. K. C. Thomas, *et al.*, Structure-activity relationship of capsaicin analogs and transient receptor potential vanilloid 1-mediated human lung epithelial cell toxicity. *J. Pharmacol. Exp. Ther.* **337**, 400–410 (2011).

75. F. Yang, J. Zheng, Understand spiciness: mechanism of TRPV1 channel activation by capsaicin. *Protein Cell* **8**, 169–177 (2017).

76. F. Yang, *et al.*, The conformational wave in capsaicin activation of transient receptor potential vanilloid 1 ion channel. *Nat. Commun.* **9**, 2879 (2018).

77. E. M. Doherty, *et al.*, Novel Vanilloid Receptor-1 Antagonists: 2. Structure−Activity Relationships of 4-Oxopyrimidines Leading to the Selection of a Clinical Candidate. *J. Med. Chem.* **50**, 3515–3527 (2007).

78. T.-Y. Liu, Y. Chu, H.-R. Mei, D. Chang, H.-H. Chuang, Two vanilloid ligand bindings per channel are required to transduce capsaicin-activating stimuli. *Front. Mol. Neurosci.* **12**, 302 (2019).

79. K. Zhang, D. Julius, Y. Cheng, Structural snapshots of TRPV1 reveal mechanism of polymodal functionality. *Cell* **184**, 5138–5150.e12 (2021).

80. L. G. Po, M. Siddiq, T. Shahzad, "Chili, Peppers, and Paprika" in *Handbook of Vegetables and Vegetable Processing*, (John Wiley & Sons, Ltd, 2018), pp. 633–660.

81. E. Blum, *et al.*, Molecular mapping of capsaicinoid biosynthesis genes and quantitative trait loci analysis for capsaicinoid content in Capsicum. *Theor. Appl. Genet.* **108**, 79–86 (2003).

82. M. Cerone, T. K. Smith, Desaturases: Structural and mechanistic insights into the biosynthesis of unsaturated fatty acids. *IUBMB Life* **74**, 1036–1051 (2022).

83. A. A. Millar, M. A. Smith, L. Kunst, All fatty acids are not equal: discrimination in plant membrane lipids. *Trends Plant Sci.* **5**, 95–101 (2000).

84. R. Q. Thompson, Homocapsaicin: nomenclature, indexing and identification. *Flavour Fragr. J.* **22**, 243–248 (2007).

85. K. Kobata, *et al.*, Long-chain N-vanillyl-acylamides from Capsicum oleoresin. *J. Agric. Food Chem.* **58**, 3627–3631 (2010).

86. R. S. S. H. li-chin, https://mzmine.github.io/mzmine_documentation/index.html. *Data handling (supported formats)* (2023). Available at: https://mzmine.github.io/mzmine_documentation/data_conversion.html.

87. H. L. Constant, G. A. Cordell, D. P. West, Nonivamide, a Constituent of Capsicum oleoresin. *J. Nat. Prod.* **59**, 425–426 (1996).

88. F. Higashiguchi, H. Nakamura, H. Hayashi, T. Kometani, Purification and structure determination of glucosides of capsaicin and dihydrocapsaicin from various Capsicum fruits. *J. Agric. Food Chem.* **54**, 5948–5953 (2006).